FRICTION-INDUCED OSCILLATIONS IN ROCK SYSTEMS

by

KWONG CHING WONG

B.Sc., National Taiwan University
Taipei, Taiwan, 1971

A THESIS SUBMITTED IN PARTIAL FULFILMENT OF

THE REQUIREMENTS FOR THE DEGREE OF

MASTER OF APPLIED SCIENCE

in the Department
of
Mechanical Engineering

We accept this thesis as conforming to the

required standard

THE UNIVERSITY OF BRITISH COLUMBIA

April, 1974

ABSTRACT

Friction-induced vibrations and the rate dependencies of friction were studied for steel, glass and four types of rock. The mathematical analysis of Cameron was modified to include a force rate parameter as used by Johannes. A new equation was used in the analysis relating the static coefficient of friction with above mentioned force rate parameter. This equation was found to be valid for each of the materials used which possessed stick-slip vibrations. Reasonable correlations were obtained between the analytical curves and the experimental data. Stick-slip vibration theory was used to explain the mechanics of shallow earthquakes. A rough calculation of the permanent displacement of the 1906 San Francisco earthquake was obtained and found to be very close to the reported value. A formula for estimating the period of the fault displacement was introduced.

TABLE OF CONTENTS

Table of contents cont.

LIST OF FIGURES

List of figures cont.

List of figures cont.

CHAPTER I

1-1. INTRODUCTION:

In recent years, new tectonic theory suggests that relative movements of adjoining blocks in the lithosphere are the results of the actions in zones of convergence and divergence . These relative movements are usually accompanied by earthquakes. Geologists suggest that faulting is an earthquake mechanism and that stick-slip vibrations might be used to explain earthquakes at shallow depth.

Stick-slip vibrations of rock have been studied experimentally by other investigators under triaxial stress conditions. Some of these studies are concerned with the so-called time dependent mechanism of static friction, but no previous studies have been concerned with the stress rate dependent characteristics of rock friction.

The present research is concerned with an investigation of the rate sensitivity of the friction and the friction induced vibrations of rock systems, especially the amplitude of stick-slip from which the intensity and periodicity of earthquakes can be estimated.

1-2. HISTORICAL:

1-2-1. ENGINEERING BACKGROUND:

When two surfaces are loaded together and subjected to a shear force, the force that resists the relative movement between these two surfaces is defined as the friction force. As the shear force is increased to a critical value, relative gross motion commences, which may take the form of vibration. The fluctuating phenomenon, when it occurs, is called friction-induced or self-excited vibration. When the displacement of the vibrating system is plotted versus time, two forms of friction-induced vibration may be observed depending on the frictional conditions. Stick-slip vibration, Fig. 1-1a, is the friction induced vibration that has a saw-tooth form curve; whereas quasi-harmonic vibration, Fig. 1-1b, is the form which has a curve similar to a sinusoidal curve.

Friction-induced vibration is a common phenomenon and occurs in a variety of situations. However, research was not commenced in this area until early in the twentieth century. In 1929, when Wells tried to measure the kinetic friction at low speed (1), he found that the displacement of his measuring system fluctuated periodically. Four years later, Kaidanovskii and Khaikin (2) suggested that there must exist a region where the slope of the friction versus velocity curve was negative if two surfaces were rubbed together to produce intermittent motion. In 1939, when Bowden and Leben (3) worked on the friction between metallic surfaces, they observed that the frictional force did not remain constant and that the motion proceeded in jerks. In 1943, Bowden, Moore and Tabor (4) suggested that friction was probably due to the welding of the surface at local points

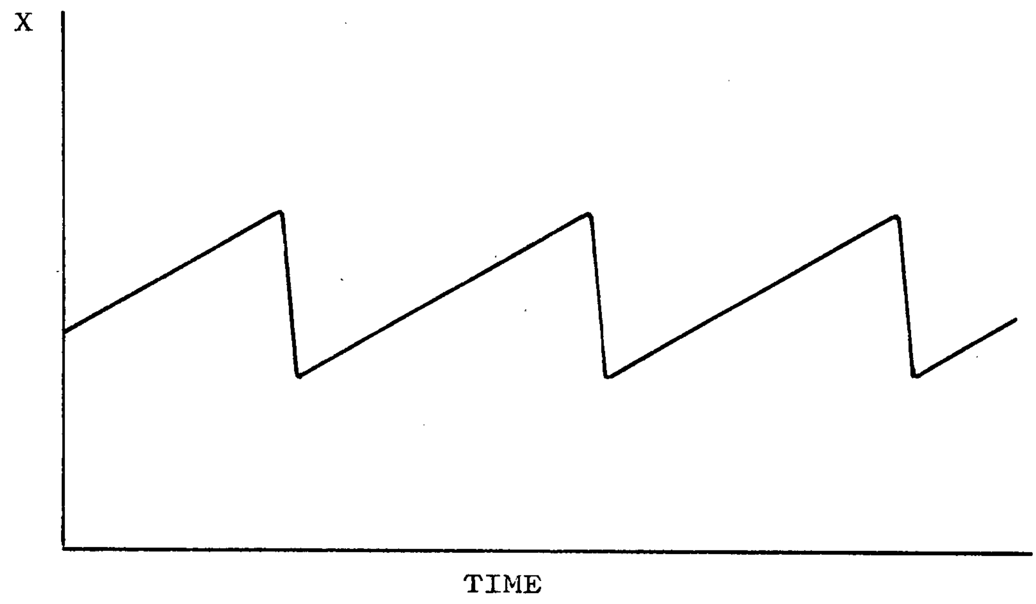

FIG. 1-1a. STICK-SLIP VIBRATIONS

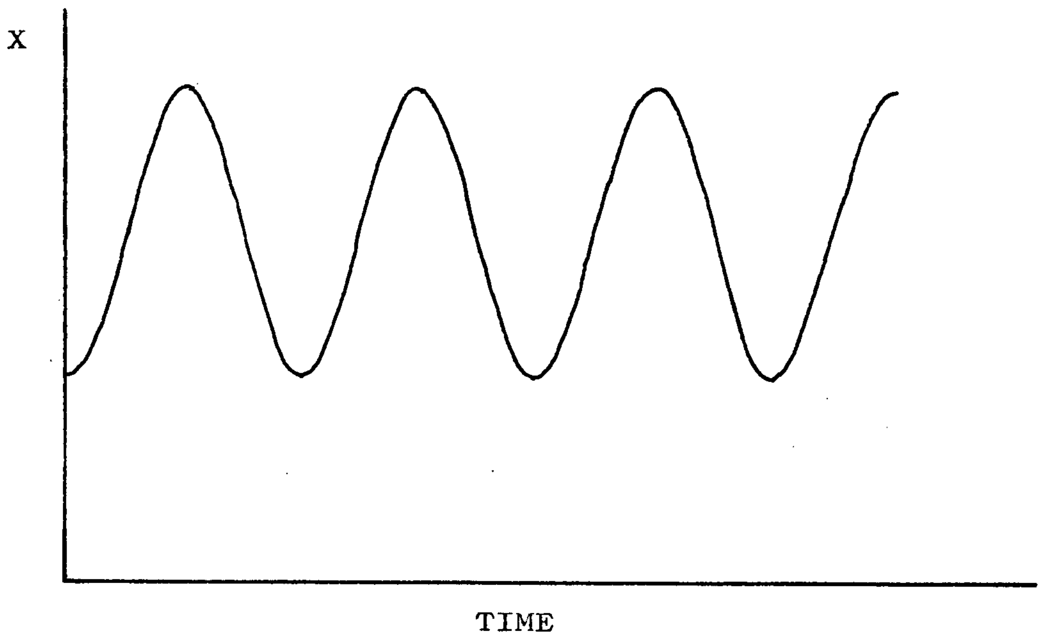

FIG. 1-1b. QUASI-HARMONIC VIBRATIONS

of contact which were plastically deformed.

In 1945, Bristow (5) confirmed that stick-slip oscillation required the existence of a region of negative slope in the friction versus velocity curve. He also pointed out that micro-displacement was observed during stick.

By using of Lienard's graphical method (6), Dudley and Swift (7), in 1949, developed a graphical technique so that any cycle of the friction-induced vibration could be plotted on a phase plane of displacement versus velocity. They predicted that the amplitude of vibration increased with increasing driving velocity.

In 1951, Rabinowicz (8) suggested that junctions increased in size with time and that as the time of stick increased the static coefficient of friction increased to a maximum. In 1957 (9), he published his experimental results which showed that the amplitude of the vibration decreased as driving velocity was increased, and the amplitude appeared to die out once the driving velocity reached a sufficiently high value.

Derjagin, Push and Tolstoi (10) provided a theoretical analysis of stick-slip vibrations. By using his analysis, Singh (11) found that reducing the difference of static and kinetic friction might be a useful way to suppress the friction-induced vibration or an increase of damping coefficient could give a similar result.

In 1962, Potter (12) observed that the amplitude of vibration decreased with increasing velocity, which was quite different from the result that Dudley and Swift (7) predicted. He also indicated that the amplitude of vibration died out at a certain point of the friction-velocity curve. One year later, Cameron (13) showed in a theoretical analysis that the amplitude of vibration and the critical velocity (the velocity when vibration died out) could be predicted.

In 1969, a new concept about the mechanics of static static friction was proposed. Johannes (14) pointed out that amplitude of vibration was not governed by time of stick, but by $\dot{\theta}$, the rate of application of the transverse shear force divided by the normal load. His conclusion was proved by Green (15), in 1971, when studying stick-slip vibration. Green reported that no obvious increase in electrical conductivity across the surfaces was observed when the rate of applying shear force was reduced to zero no matter what length of time was involved. This finding suggested that the area of contact did not depend on the time of contact.

In 1972, Marion (16) suggested that plastic deformation was the governing mechanism of contact growth, and that there was an upper asymptote for the μ_s-$\dot{\theta}$ curves for metals.

1-2-2. GEOLOGICAL BACKGROUND:

The first earthquake was recorded about 4000 years ago and was attributed to supernatural forces. In about 350 B.C., Aristotle (17) classified earthquakes into six types according to the nature of the earth movement observed. In

132 A.D., Chang Heng (17) made an instrument which indicated the direction of the first impulse of an earthquake.

In the middle of the nineteenth century, Robert Mallet (17) suggested a world wide systematic observatory chain. Up to the end of that century, several ideas were suggeated as the cause of earthquakes (18) including the outbreak of volcanoes, the formation of mountains, the collapse of mountains, explosions, upheaval and downthrow of mountains, and the most striking one —— the sudden snapping under an elastic strain. This latter proposal led Reid (19), in 1911, to introduce his elastic rebound theory after he had studied the San Francisco earthquake of April 18,1906.

In the early twentieth century the growth of internal stress leading up to fracture (20) was believed to be the mechanism of earthquakes. This concept is very close to the shallow earthquake mechanism accepted by most contemporary geologists.

In 1910, Taylor (21) and Wegener (22) pointed out the similarity in shapes and geology of several adjacent coasts and introduced the striking hypothesis of continental drift which suggested that those similar adjacent coasts were formerly united and that the continent had moved apart. The movements would be associated with fracture of the earth's crust. Bernal, Dietz and Hess (23) suggested that convection currents in the mantle rose and seperated under the mid-ocean ridges, and that sea floor spreading was associated with this concept. The Taylor and Wegener hypothesis of continental drift, the Dietz and Hess theory of sea floor spreading, coupled with the suggestion of transform fault and underthrusting of the lithosphere at the island arcs, provided the basis for a new global tectonic theory which was introduced by Isacks, Oliver and Sykes (24) in 1968. This theory provided an explanation of the entire mechanism of the formation of the continents and oceans of the Earth. In addition, shear forces produced at transform faults and island arcs could be explained.

In 1959, Orowan (25) suggested that earthquakes due to fracture or friction-sliding could only occur at focal depths less than ten kilometers, and that shear melting and faulting should be the mechanism of deep focus earthquakes. His theory was based on the idea that stress and temperature at increased depths in the earth's crust were so high that flow rather than fracture occurred.

Jaeger (26), in 1959, observed stick-slip vibration in his laboratory experiments with porphyry rocks. Griggs et al (27), in 1960, found that stick-slip often occurred with single crystals of silicate minerals. Bridgman (28), in 1960, worked on the shearing phenomena of over 200 inorganic compounds at high pressure and he found that the shear phenomena of a few showed evidence of stick-slip behaviour.

In 1966, Brace and Byerlee (29) pointed out that at depths less than 25 kilometers, friction-sliding might be the mechanism of earthquakes and that earthquakes could be considered to be large-scale stick-slip. They noted that the majority of destructive earthquakes in California and Japan occurred at this shallow depth. In 1968 (30), they concluded from their experimental results that the amplitude of stick-slip was independent of strain rate, stiffness and elastic properties of surroundings. These findings are surprising in the light of current knowledge concerning stick-slip. In 1970 (31), they pointed out that the sliding was unstable at high pressure and at low temperature, and stable at low pressure and at high temperature.

Drennon and Handy (32), in 1971, made a series of experiments to investigate the stick-slip of limestone. They showed that stick-slip was not limited to quartz-rich rock, and that friction depended upon temperature and normal load, and that the previous frictional history of the specimen is critical in the initiation of stick-slip. Dieterich (33), in 1972, reported that friction in rocks was time dependent, but he did not provide any stick-slip results to substantiate this observation.

The foregoing review of previous research suggested that more work on the frictional phenomena of rocks was required. The purpose of the present work was to study the friction and friction induced vibration of rock systems with special reference to the parameter $\dot{\theta}$, the rate of applying shear force divided by normal load.

CHAPTER II

THEORY

The present theoretical analysis is an extension of the work of Cameron. Cameron assumed that the static coefficient of friction was dependent of time of stick, whereas, Jobannes introduced a load rate parameter, $\dot{\theta}$, and suggested that the static coefficient of friction depended upon $\dot{\theta}$ rather than time of stick. The modification of the theory produced by the Johannes concept of static friction is considered.

THEORETICAL ANALYSIS:

Consider a vibrational system which consists of a mass M, a spring with stiffness K and a dash pot with damping coefficient C as shown in Fig. 2-1. Assume that the mass of the lower platform is very much higher than that of the slider M, and that the platform moves with a velocity V with respect to the datum. That is, any motion of M will not affect the movement of the platform.

When the slider is in its equilibrium position and V is zero, forces on the spring and the dash pot are zero as well as the shear force, F_f, between M and the platform. The displacement, x, of the slider is measured from this equilibrium position. If the coefficient of friction, μ, between M and the platform is not zero, the mass

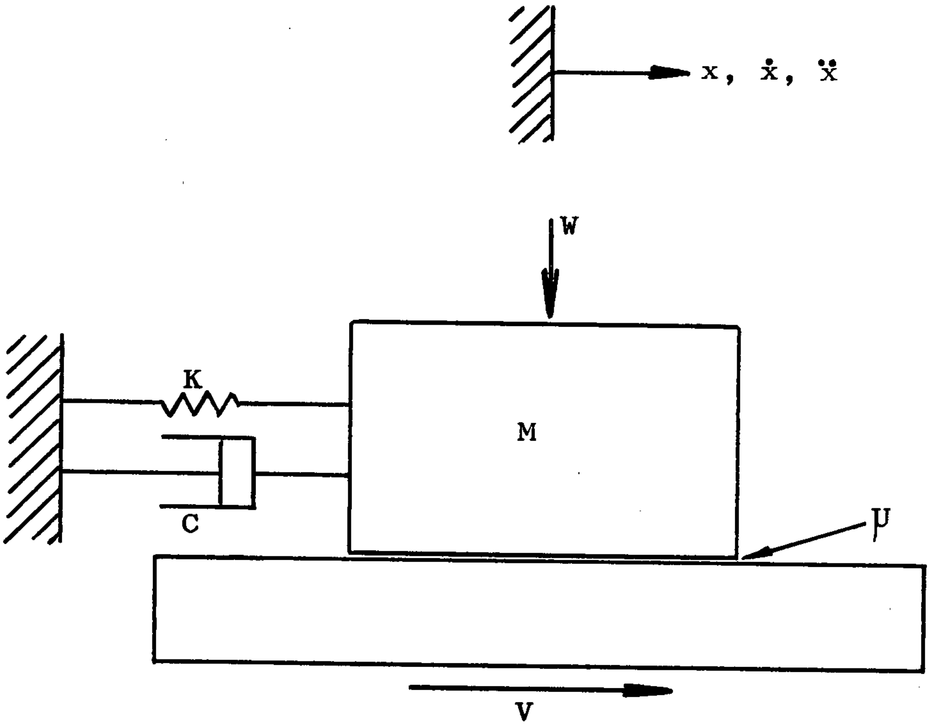

FIG. 2-1. MODEL OF THE SLIDING SYSTEM

M will stick to the platform when the platform is moving with velocity V. This situation will last until the resultant force of the spring and the dash pot equals the shear force. Then, if the platform moves slightly further, gross relative motion between the mass and the platform starts to occur.

During the stick period, in which relative motion is almost zero, the motion of the slider can be expressed as:

$$Kx + C\dot{x} + M\ddot{x} = W\mu_s \qquad (2-1)$$

where W is normal load and is equal to Mg in the present system.

Assume that the velocity of the platform is constant, i.e.

$$\dot{x} = V = \text{Constant}$$

Therefore,

$$\frac{dV}{dt} = \frac{d\dot{x}}{dt} = \ddot{x} = 0$$

Equation (2-1) becomes:

$$Kx + C\dot{x} = W\mu_s \qquad (2-2)$$

$\dot{\theta}$ is defined as the rate of applying the shear force divided by the normal load acting on the surface.

Assume that W is time independent.

$$\dot{\theta} = \frac{d}{dt}\left(\frac{F_f}{W}\right) = \frac{\dot{F}_f}{W}$$

From equation (2-2):

$$\dot{F}_f = \frac{d}{dt}(Kx + C\dot{x})$$

$$= K\dot{x} + C\ddot{x}$$

$$= K\dot{x} \qquad \text{for } \ddot{x} = 0$$

$$= KV$$

Therefore,

$$\dot{\delta} = \frac{KV}{W} \tag{2-3}$$

At the instant when the slider starts to slip, that is at the end of stick period, the shear force at the contact surface is equal to the static friction force.

$$Kx + C\dot{x} = W\mu_s \tag{2-4}$$

Consider the case where $\dot{x}$ and C are very small whereby the term $C\dot{x}$ in equation (2-4) becomes negligible, then,

$$Kx = W\mu_s$$

or $$\mu_s = \frac{Kx}{W} \tag{2-5}$$

During the slip portion of the cycle the motion of the slider is no longer the same as the platform. Consider the governing equation in this situation:

$$Kx + C\dot{x} + M\ddot{x} = W\mu \tag{2-6}$$

where $\dot{x} \neq V, \quad \ddot{x} \neq 0$

and μ is the kinetic coefficient of friction of the sliding system and is usually a non-linear function of velocity.

The necessary condition that frictional vibrations occur is that there must exist a region of negative slope in the friction-velocity curve.

Consider a μ-velocity curve with positive slope as shown in Fig. 2-2, with μ_s occurring at the lowest point of the curve. System having a μ-V curve similar to this will achieve steady sliding motion throughout the whole velocity region. Friction induced vibration will not commence

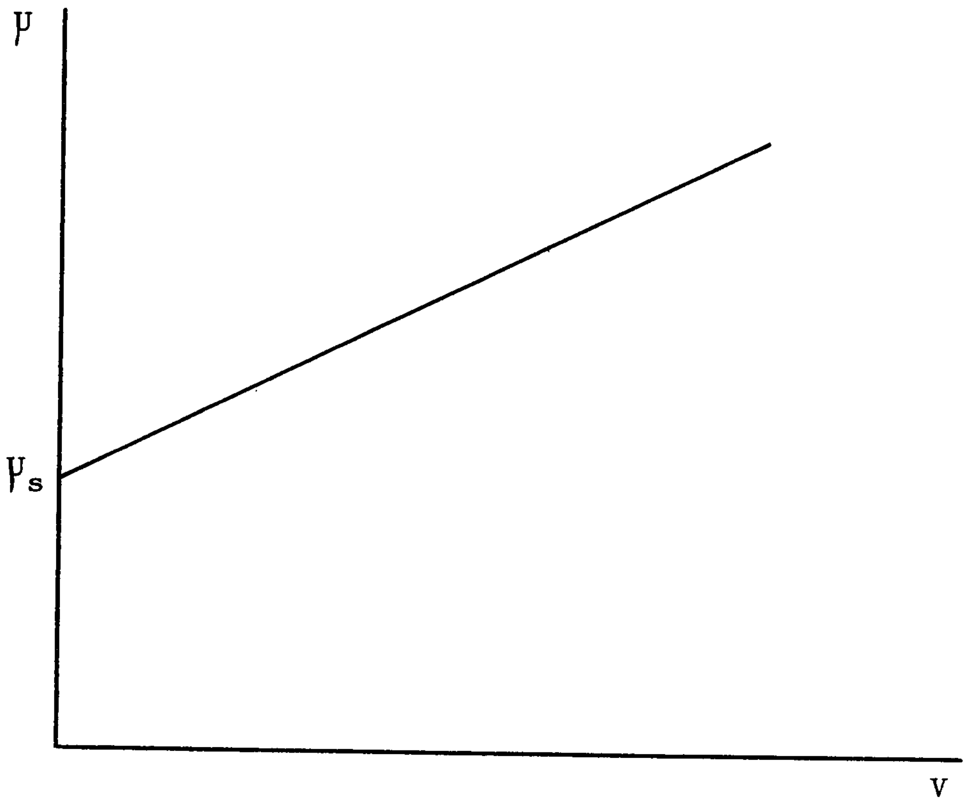

FIG. 2-2 μ-V CHARACTERISTIC CURVE OF A POSITIVE SLOPE FORM because build-up of frictional resistance in opposition to the applied force is impossible.

A second form of μ-V curve, similar to Fig. 2-2, but baving a region of negative slope in the low velocity region is shown in Fig. 2-3. It is believed that the μ-V curve in Fig. 2-3 describes the friction behaviour of most materials. Stick-slip vibration occurs in the low velocity region and diminishes as velocity is increased.

Ko (34) pointed out that quasi-harmonic vibration existed when the μ-V curve assumed the form shown in Fig. 2-4. It was found that materials possessing quasi-harmonic oscillations often show stick-slip oscillations in the low velocity region. A μ-V curve descriptive of the general frictional behaviour of materials is shown by Fig. 2-5.

A typical friction-velocity curve for stick-slip oscillations is shown in Fig. 2-3 which is linearized as shown in Fig. 2-6. This linearized μ-V relationship can be expressed as:

$$\mu = \mu_m + \beta(V - \dot{x}) \qquad (2\text{-}7)$$

Equation (2-6) can be linearized with the help of Fig. 2-6. Put equation (2-7) into equation (2-6):

$$Kx + C\dot{x} + M\ddot{x} = W(\mu_m + \beta V - \beta\dot{x})$$

i.e.:

$$Kx + (C + \beta W)\dot{x} + M\ddot{x} = W(\mu_m + \beta V) \qquad (2\text{-}8)$$

Define:

$$\zeta = \tfrac{1}{2}(C + \beta W)(KM)^{-\frac{1}{2}}$$

$$\omega_d = \omega_n(1 - \zeta^2)^{\frac{1}{2}}$$

$$\lambda = \zeta(1 - \zeta^2)^{-\frac{1}{2}}$$

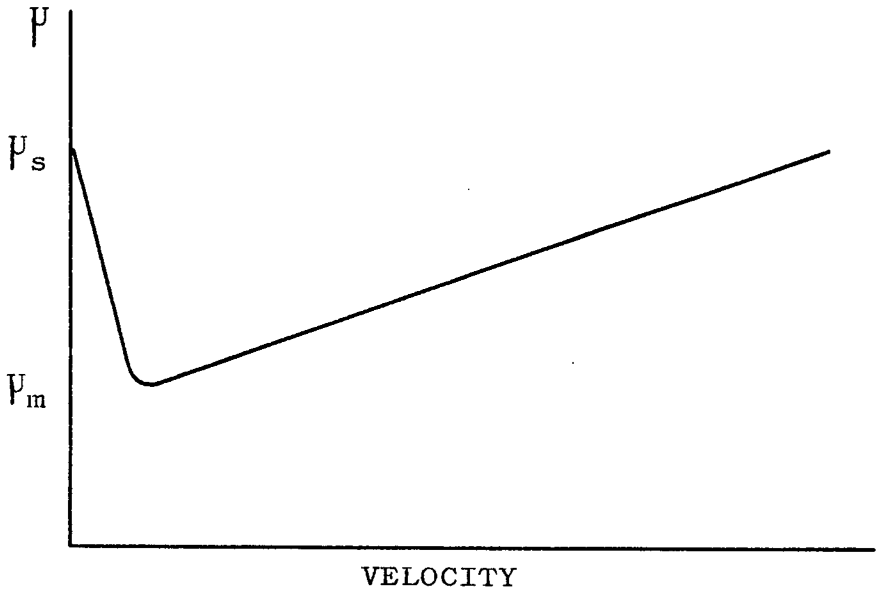

FIG. 2-3 μ-V CHARACTERISTIC CURVE OF A NEGATIVE SLOPE AT LOW VELOCITY REGION

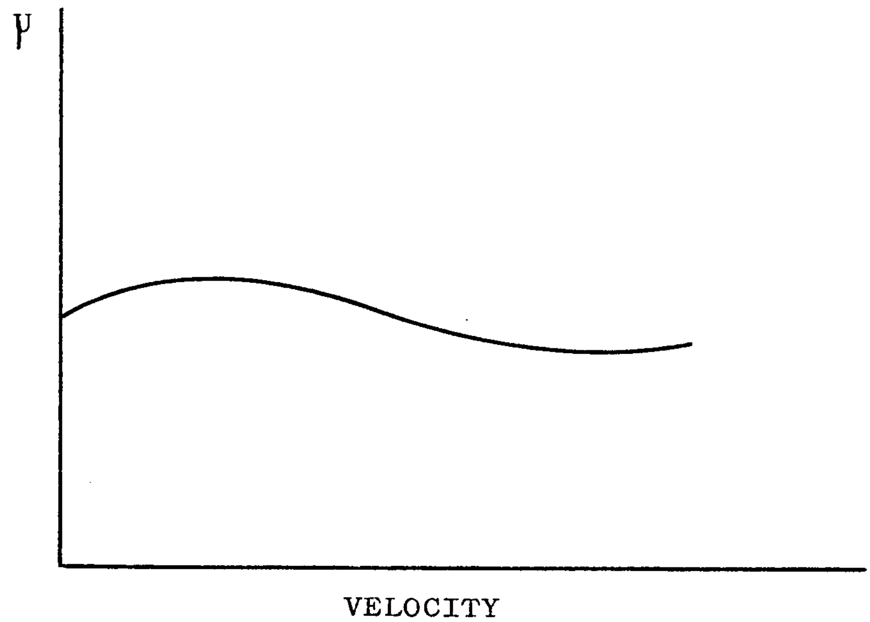

FIG. 2-4 HUMPED FORM OF A μ-V CHARACTERISTIC CURVE

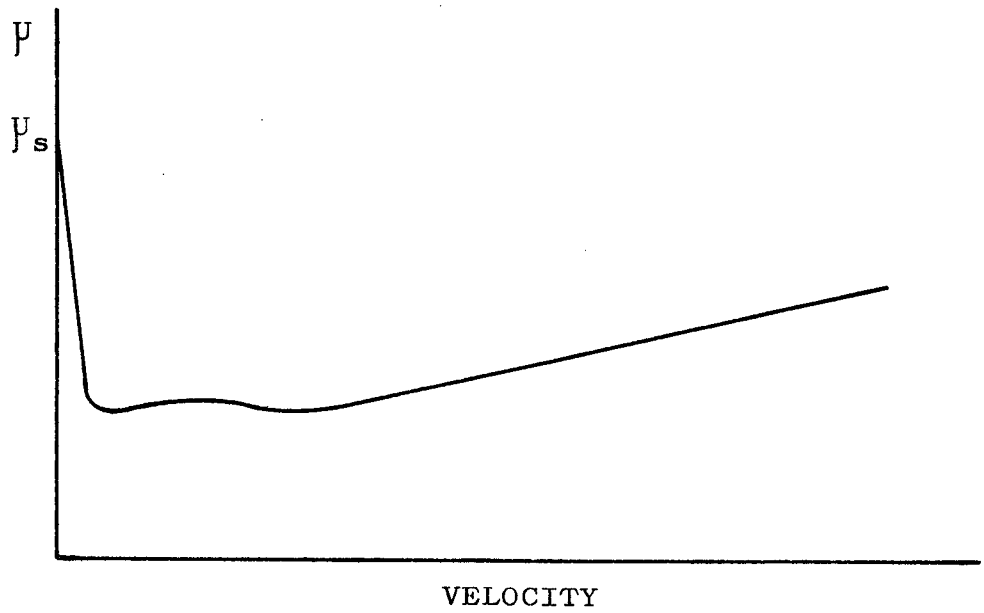

FIG. 2-5 POSSIBLE FORM OF μ-V CHARACTERISTIC CURVE

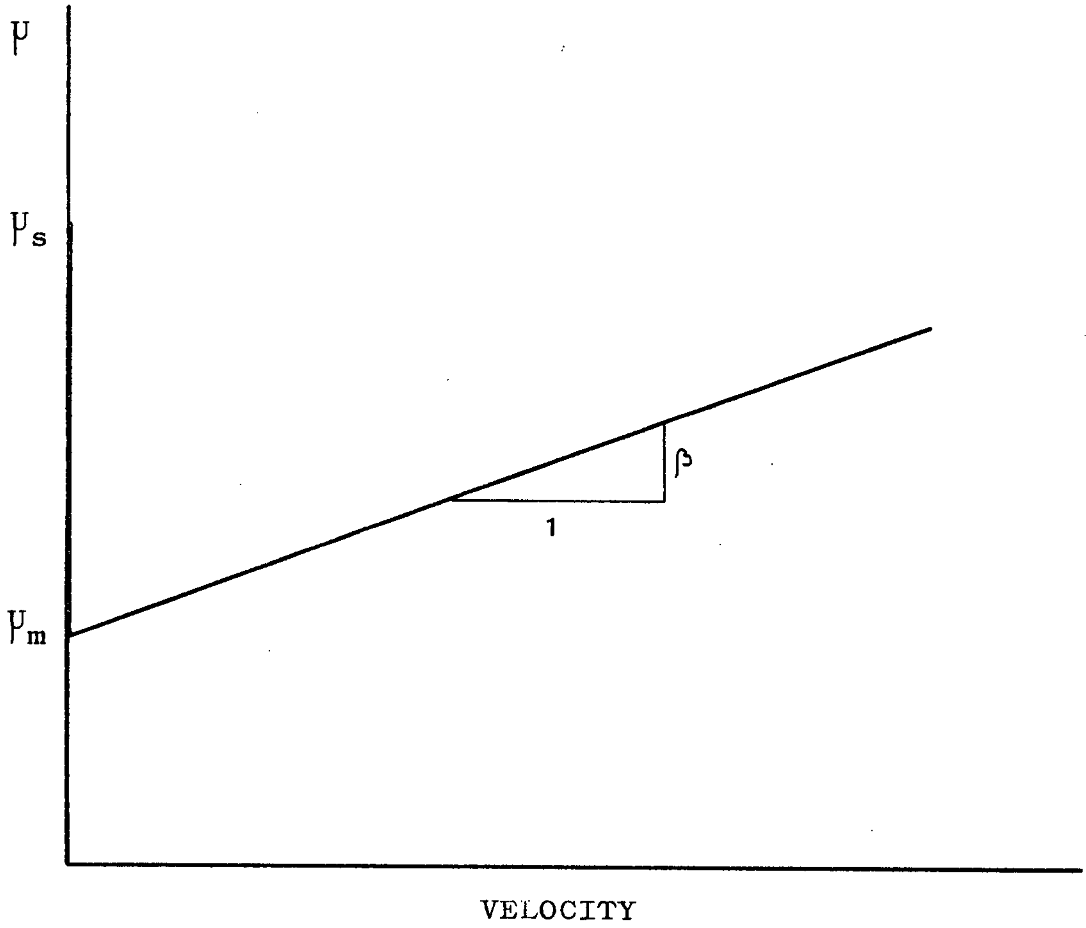

FIG. 2-6 LINEARIZED μ-V RELATIONSHIP CURVE

A standard solution to equation (2-8) is:

$$x = \frac{W}{K}(\mu_m + \beta V) + e^{-\lambda\omega_d t}\left[A\cos\omega_d t + B\sin\omega_d t\right] \quad (2\text{-}9)$$

The first derivative of x gives:

$$\dot{x} = \omega_d e^{-\lambda\omega_d t}\left[(B - \lambda A)\cos\omega_d t - (A + \lambda B)\sin\omega_d t\right] \quad (2\text{-}10)$$

The second derivative of x gives:

$$x = -\omega_d^2 e^{-\lambda\omega_d t}\left\{\left[A(1 - \lambda^2) + 2\lambda B\right]\cos\omega_d t + \left[B(1 - \lambda^2) - 2\lambda A\right]\sin\omega_d t\right\} \quad (2\text{-}11)$$

A solution of equation (2-8) can also be presented on a phase-plane as shown in Fig. 2-7 (14,34).

In equation (2-8)

$$Kx + (C + \beta W)\dot{x} + M\ddot{x} = W(\mu_m + \beta V)$$

let $\dot{x} = y$,

or $\ddot{x} = y\frac{dy}{dx}$

Equation (2-8) becomes:

$$Kx + (C + \beta W)y + My\frac{dy}{dx} = W(\mu_m + \beta V) \quad (2\text{-}12)$$

Setting $\frac{dy}{dx} = 0$, this gives the zero slope isocline curve.

$$x = \frac{W}{K}(\mu_m + \beta V) - \frac{1}{k}(C + \beta W)y \quad (2\text{-}13)$$

For various driven velocities, the trajectory changes. Fig. 2-8 shows three trajectories each with a zero slope isocline curve. Fig. 2-8a showa a limit cycle at low V and Fig. 2-8b showa the cycle at critical V. At a velocity higher than critical V, as shown in fig. 2-8c, the trajectory ceases to meet $\dot{x}$ = V line and spirals into an equilibrium situation. Obviously, stick-slip vibrations can only exist at a velocity lower than or equal to the

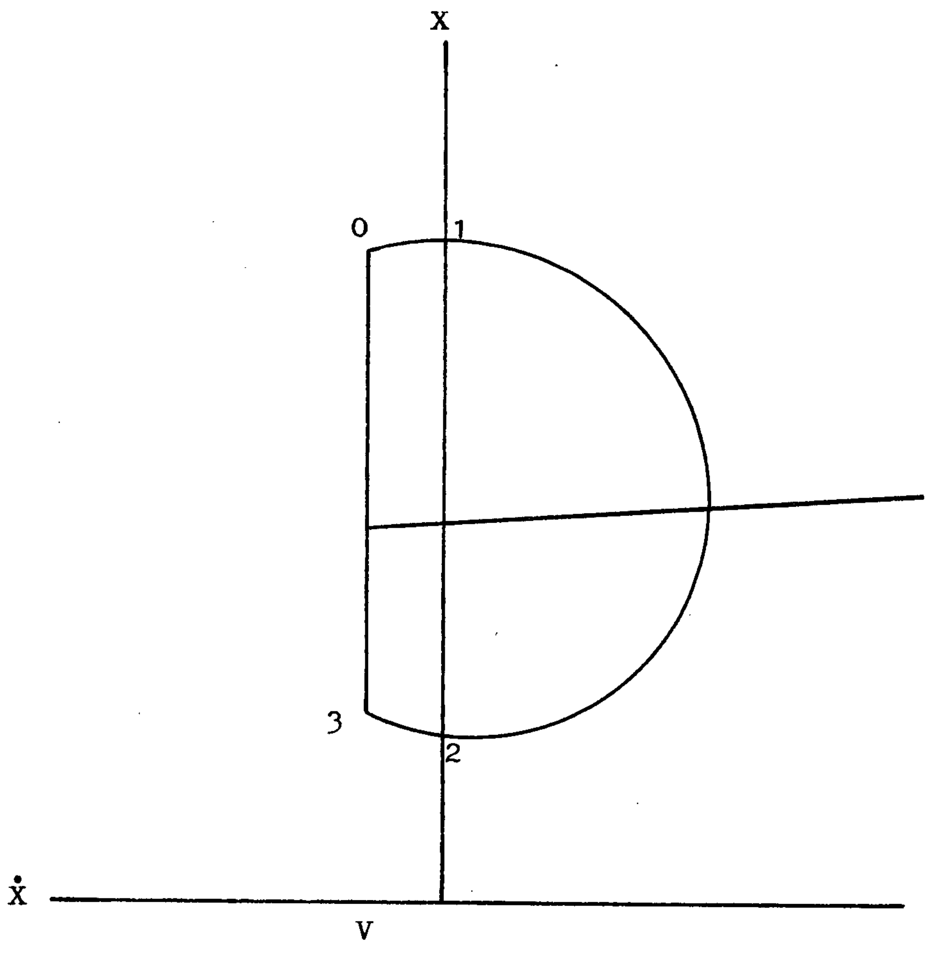

FIG. 2-7 PHASE DIAGRAM OF A STICK-SLIP CYCLE

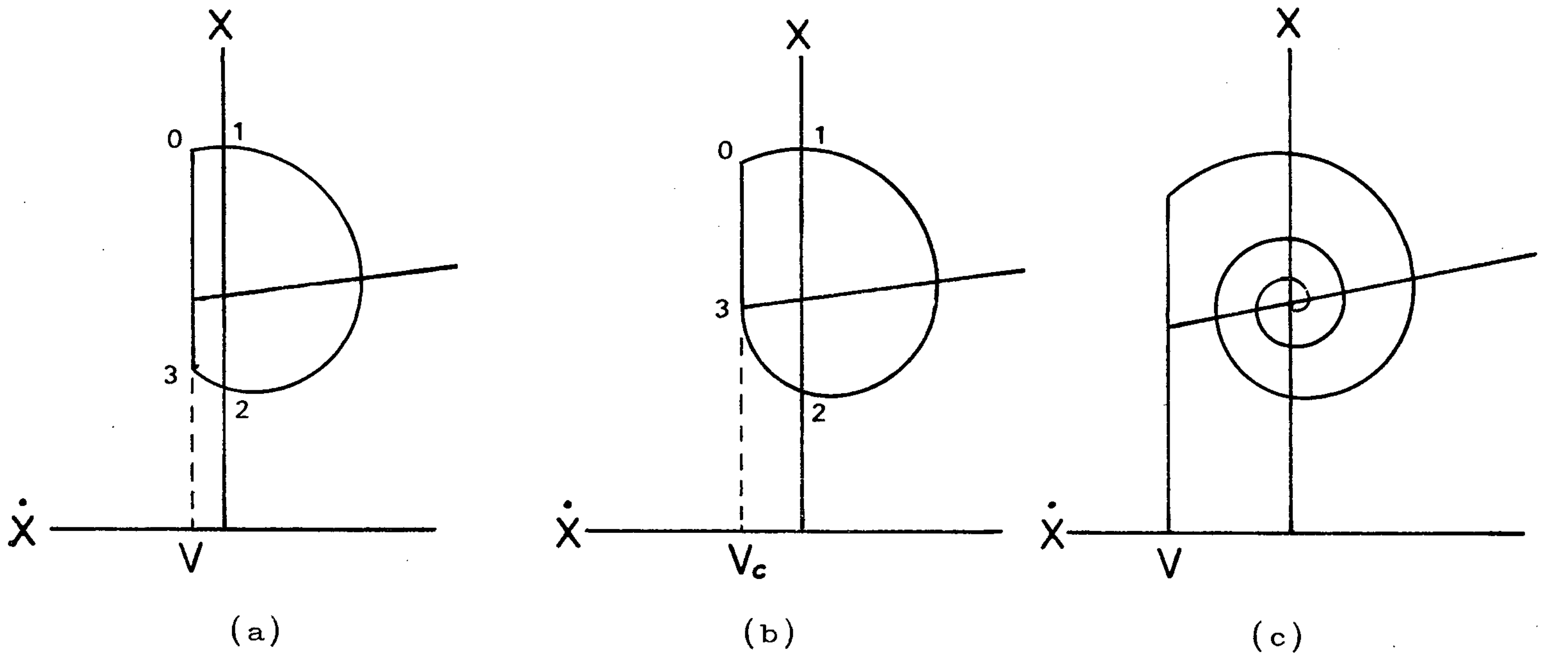

FIG. 2-8 PHASE PLANE DIAGRAMS AT DIFFERENT DRIVEN VELOCITIES

critical value. The conditions necessary for the extinction of the vibration at the critical condition are considered in Appendix I.

As an approximate treatment consider the case when the driven velocity approaches zero, that is as $\dot{\theta} \longrightarrow 0$. At V = 0, point 0, in Fig. 2-7, coincides with point 1, and point 3 coincides with point 2 as shown in Fig. 2-9.
From equation (2-5),

$$x_1 = \frac{W}{K}\mu_{so}$$

Where μ_{so} is the static coefficient of friction at V = 0.
Equation (2-9), with $t_0 = t_1 = 0$, yields

$$x_1 = \frac{W}{K}\mu_m + A$$

Therefore,

$$A = \frac{W}{K}(\mu_{so} - \mu_m) \qquad (2\text{-}14)$$

At point 2 in Fig. 2-10, $t_2 = \dfrac{\pi}{\omega_d}$,
therefore,

$$x_2 = \frac{W}{K}\mu_m - e^{-\lambda\pi}\left[\frac{W}{K}(\mu_{so} - \mu_m)\right] \qquad (2\text{-}15)$$

Let α be the amplitude of the vibration given by

$$\begin{aligned} \alpha &= x_1 - x_2 \\ &= \frac{W}{K}\mu_{so} - \frac{W}{K}\mu_m + e^{-\lambda\pi}\left[\frac{W}{K}(\mu_{so} - \mu_m)\right] \\ &= \frac{W}{K}(\mu_{so} - \mu_m)(1 + e^{-\lambda\pi}) \end{aligned} \qquad (2\text{-}16)$$

To calculate the amplitude of the vibration at a velocity other than zero, assume:

$$x_o = x_1$$

$$t_2 = \frac{\pi}{\omega_d}$$

In fact, the velocity during slip is so much higher than the driven velocity that the driven velocity can be

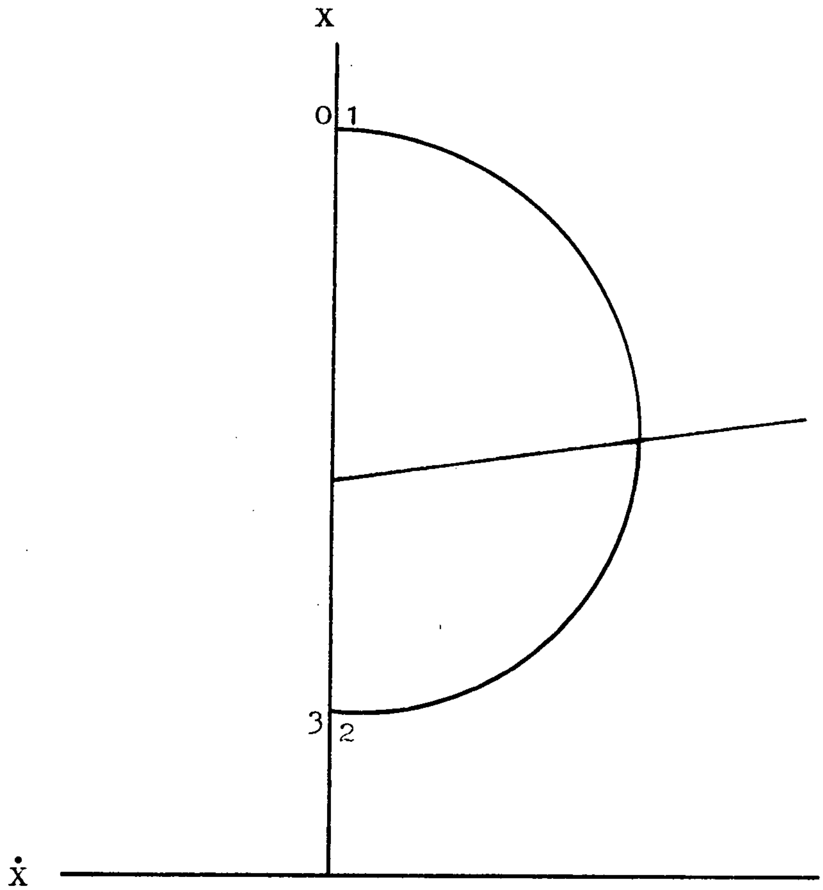

FIG. 2-9 PHASE DIAGRAM OF STICK-SLIP AT V = 0

neglected when plotted on a displacement-velocity diagram. The error arising from this assumption is very small.

Equation (2-16), therefore, can be applied to calculate the amplitude of the vibration.

$$\alpha = \frac{W}{K}(\mu_s - \mu_m)(1 - e^{-\lambda\pi}) \tag{2-17}$$

Concerning the experimental results of previous work, a μ_s-$\dot{\theta}$ curve as shown in Fig. 2-10 is introduced. The curves in Fig. 2-10 can be expressed as:

$$\mu_s = \frac{1}{\frac{1}{\mu_{so} - \mu_m} + b\dot{\theta}^d} + \mu_m \tag{2-18}$$

Equation (2-17) becomes:

$$\alpha = \frac{W}{K}\left(\frac{1}{\frac{1}{\mu_{so} - \mu_m} + b\dot{\theta}^d}\right)(1 + e^{-\lambda\pi}) \tag{2-19}$$

Knowing all the parameters of the vibrating system the amplitude of vibration can be calculated from equation (2-19).

If $V \rightarrow 0$, i.e. $\dot{\theta} \rightarrow 0$, equation (2-19) becomes:

$$\alpha = \frac{W}{K}\left(\frac{1}{\frac{1}{\mu_{so} - \mu_m} + b0^d}\right)(1 + e^{-\lambda\pi})$$

$$= \frac{W}{K}(\mu_{so} - \mu_m)(1 + e^{-\lambda\pi})$$

which is the same as equation (2-16) at $V \rightarrow 0$.

When $V \rightarrow \infty$, $\dot{\theta} \rightarrow \infty$, and clearly from equation (2-19)

$$\alpha \rightarrow 0$$

and the amplitude approaches zero at a very high driven velocity.

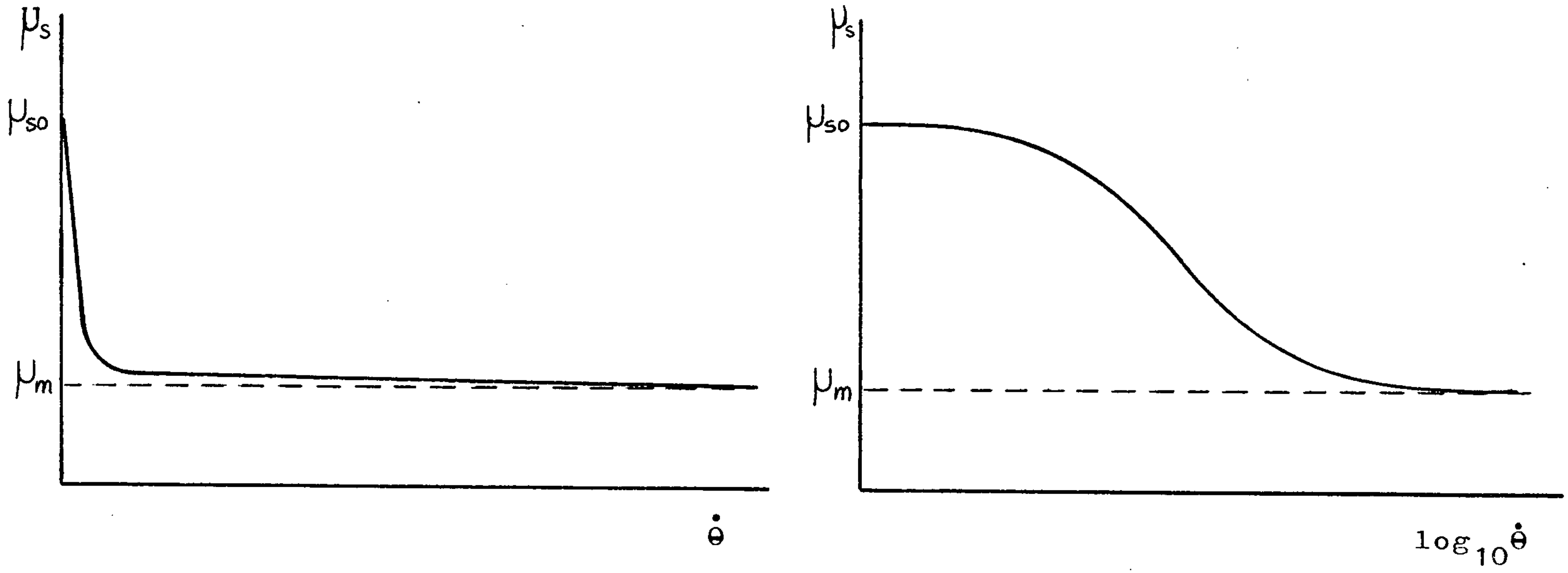

FIG. 2-10 μ-$\dot{\theta}$ CURVE AS IN EQUATION (2-18) if $\mu_{so} - \mu_m = 0$, then clearly from equation (2-19)

$$\alpha = 0$$

This latter result agrees with the suggestion of Kaidanovskii, Khaikin and Sinclair and others, that the necessary condition for the existence of intermittent motion is a region of negative slope in the friction-velocity curve.

CHAPTER III

3-1. EXPERIMENTAL APPARATUS:

The rate of displacement at the fault zones in the San Andreas fault has been reported (35) to be about 2 inches per year, or 6 X 10^{-8} inches per second. Accordingly, the frictional characteristics of rock surfaces at very low driven velocities is meaningful in the study of earthquake mechanisms. A driven velocity as low as 10^{-6} inches per second can be achieved in an hydraulically driven apparatus.

The hydraulic unit of the apparatus used in the present research consisted of a hydraulic cylinder which drove a sliding platform as shown in Fig. 3-1 and schematically in Fig. 3-2. An electrically driven, tilted axis, piston-type, constant displacement pump was used in the hydraulic supply system. An accumulator was used in the system which acted as a pulse eliminator and as a pressure reservoir. The maximum working pressure of the accumulator was 2000 psig with a capacity large enough so that the pressure could drive the piston back and forth for about five times over a length of 15 inches.

At the entrance to the cylinder a four way valve was used to control the direction of piston movement. Between the cylinder and the four way valve, 0.25 inch needle valves were placed at each end of the cylinder. These needle valves were used to give precise control of the piston movement. When the needle valves were fully opened

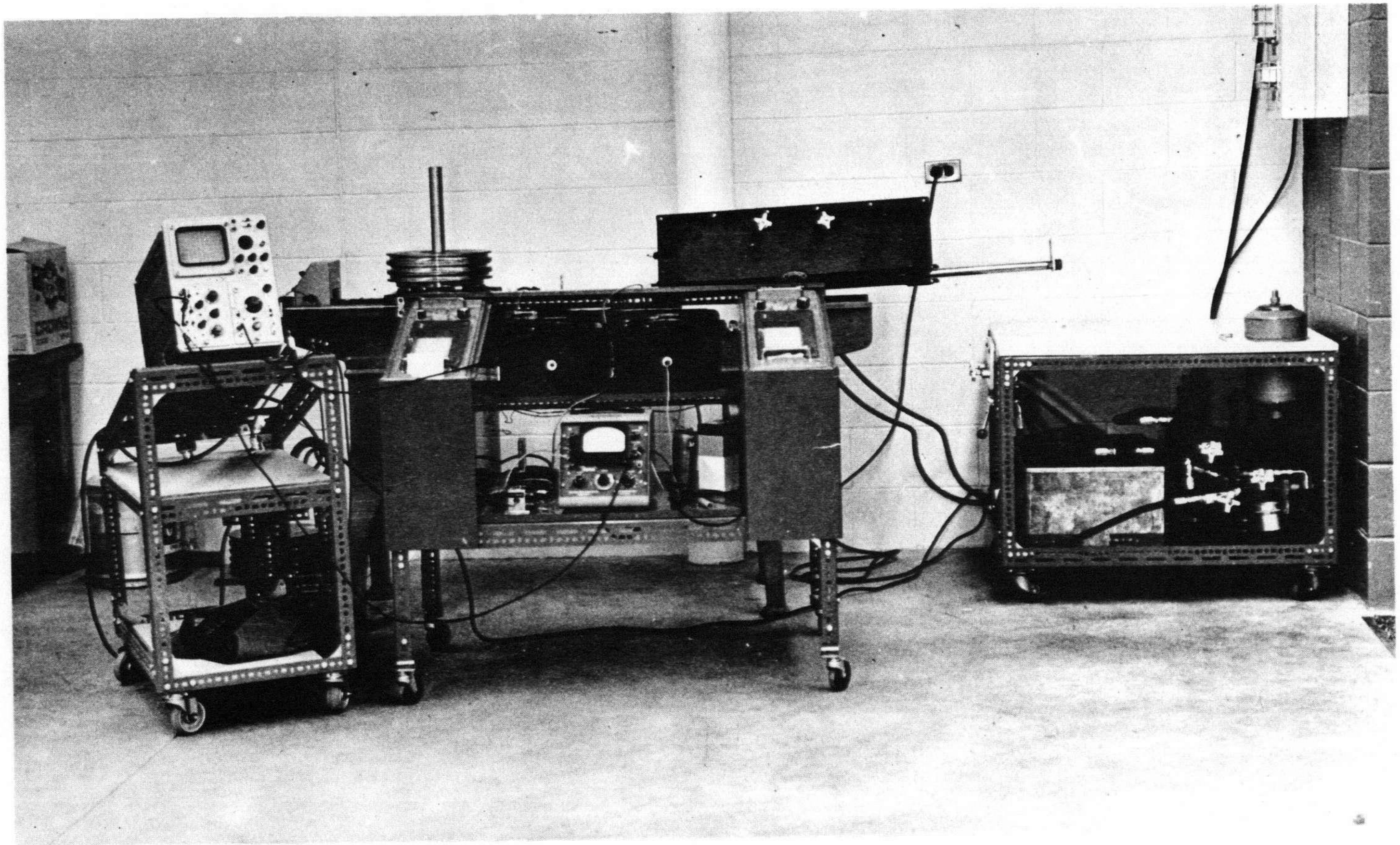

FIG. 3-1a THE ARRANGEMENT OF APPARATUS AND INSTRUMENTATION

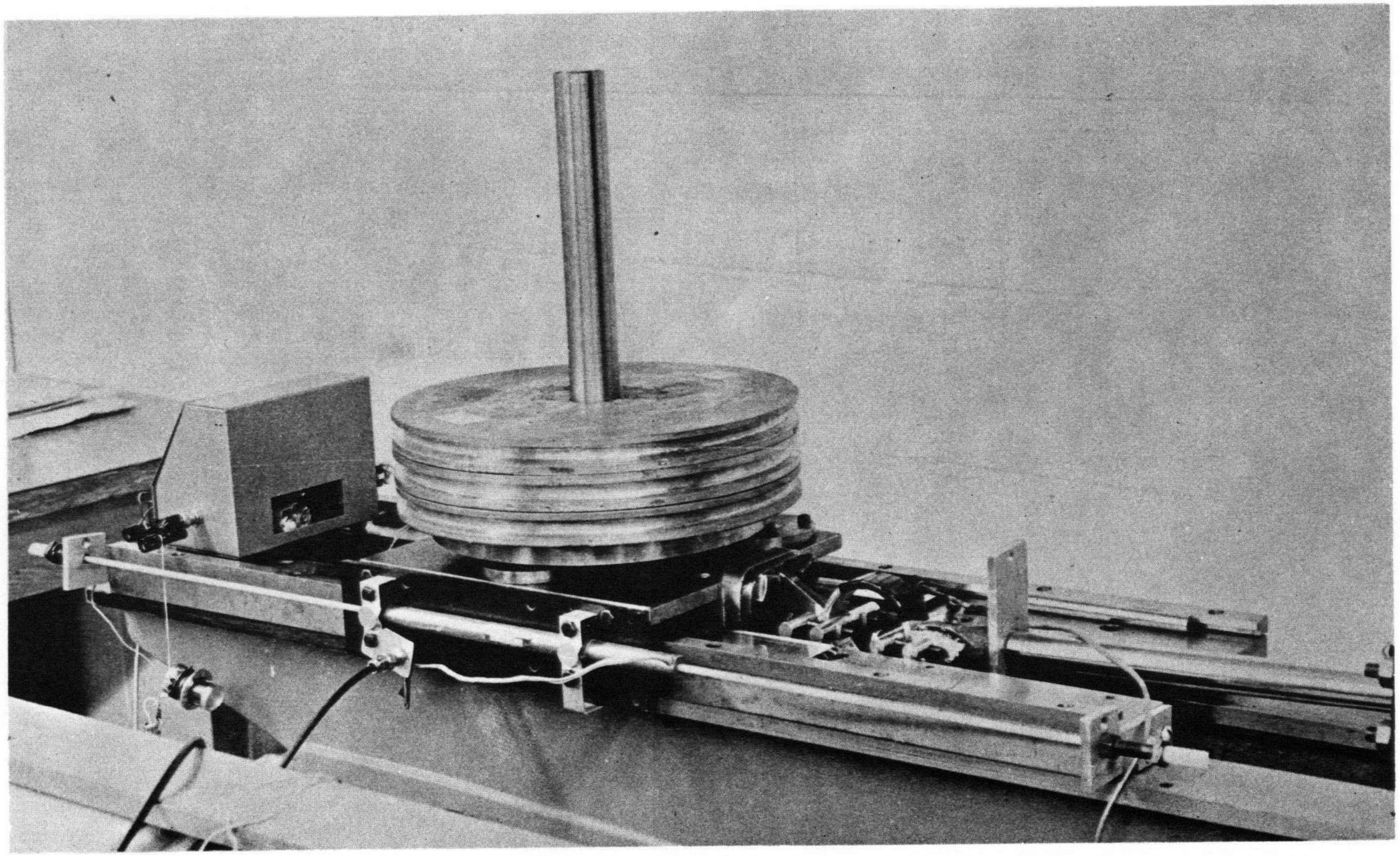

FIG. 3-1b CLOSE-UP VIEW OF APPARATUS

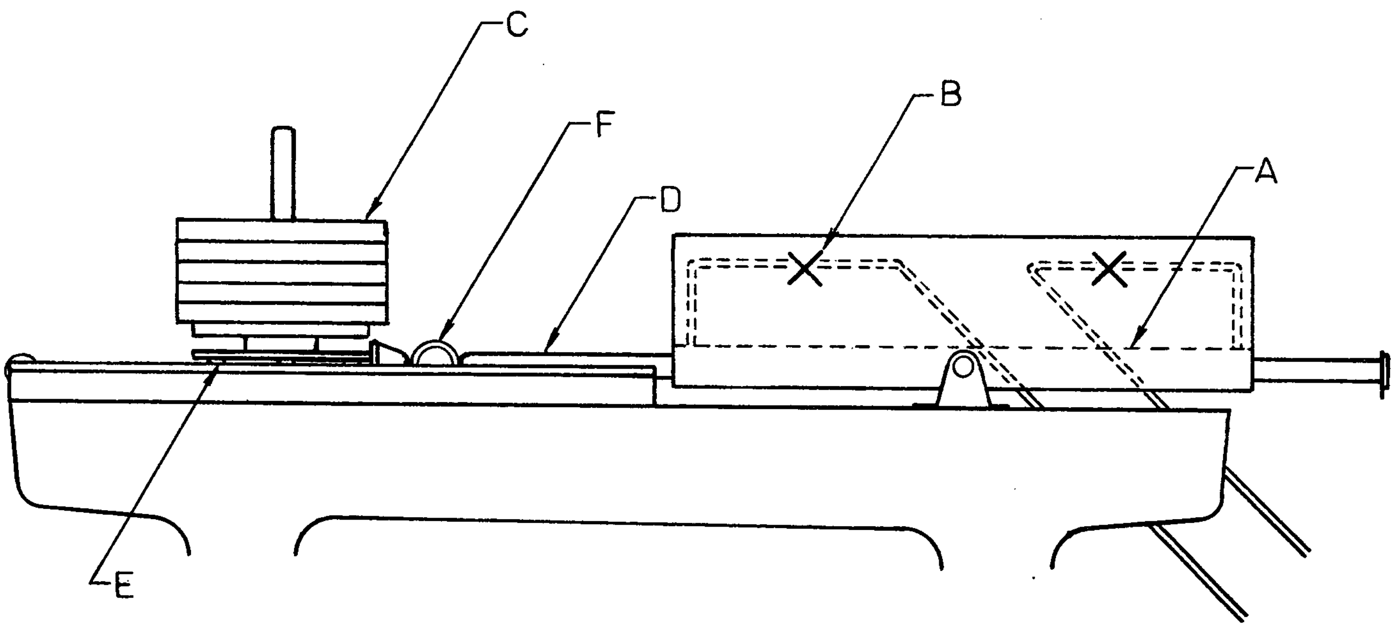

FIG. 3-2 SCHEMATIC DIAGRAM OF THE APPARATUS
A. HYDRAULIC CYLINDER, B. NEEDLE VALVE
C. LEAD WEIGHTS, D. PISTON ROD
E. SLIDERS, F. STRAIN RING

a speed of two inches per second could be obtained; when the needle valves were almost closed, a speed as low as 10^{-6} inch per second could be achieved. Oil was returned to a 15 gallon oil tank through the four way valve.

The hydraulic cylinder which had a 24 inch stroke, a 1.5 inch bore and a 1 inch diameter piston rod was mounted on a lathe bed by centrally located ball bearing pillow blocks. This mounting arrangement assisted in solving the alignment problem. The needle valves were attached on a panel secured to the cylinder. All other parts of the hydraulic system were mounted on a four-wheel cart in order to seperate the pressure source from the vibration system. Rubber wheels were used to isolate the vibration produced by the electric motor and the oil pump. Flexible hoses were used between the four way valve and the needle valves so that the cart could be moved freely. The configuration and the arrangement of the system is shown in Fig. 3-3.

The stationary specimens were blocks 2 inches wide, 0.5 inch thick and 10 to 20 inches long. These blocks were clamped to the lathe bed. Three sliders were used to support a platform. A suspension device similar to a ball and socket joint was located between the platform, as shown in Fig. 3-4, so that a small degree of tilting of the platform was allowed without affecting the contact of the sliders and rails.

The platform, which weighed 24 pounds, was connected to the piston rod of the hydraulic cylinder by a strain-ring

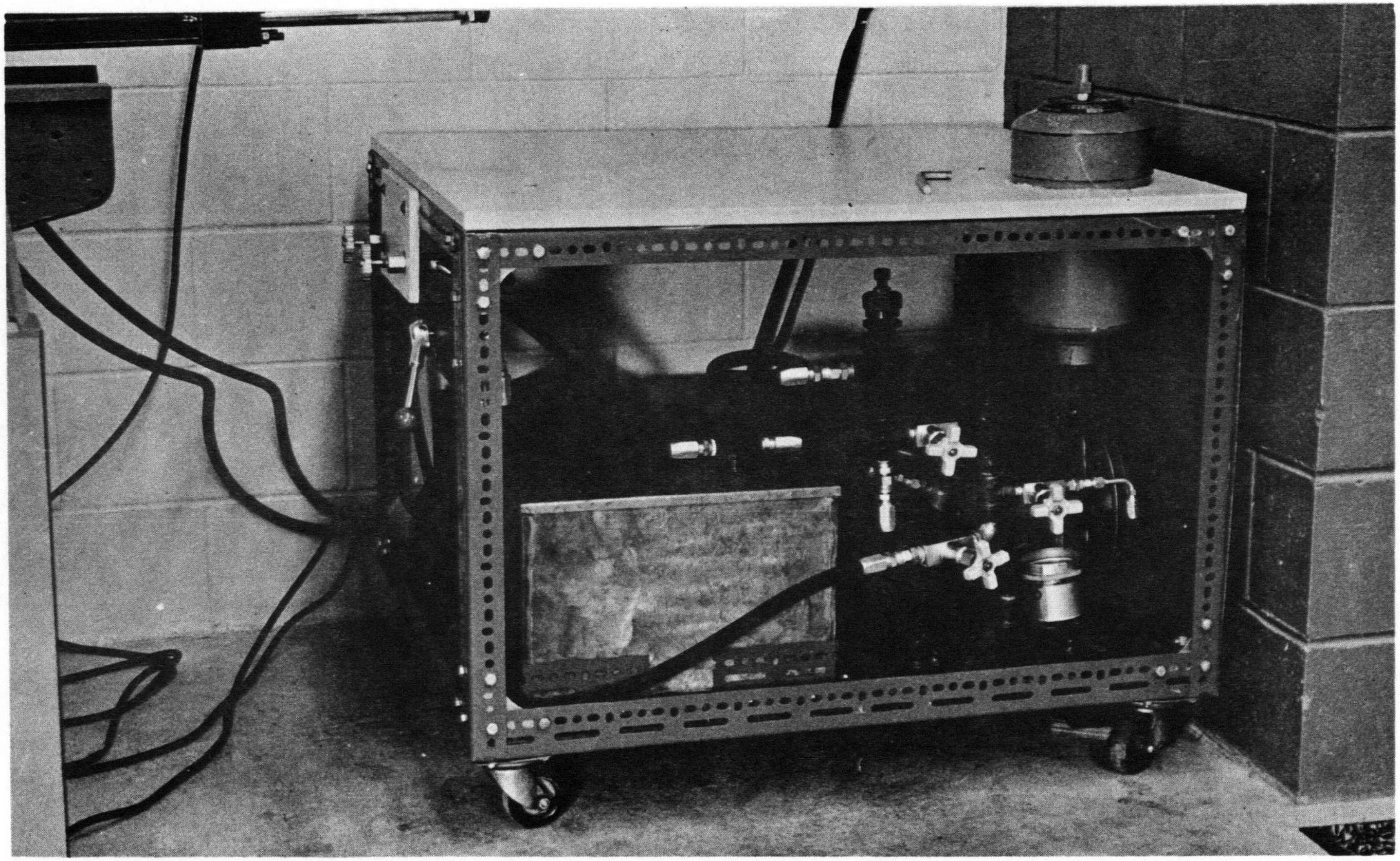

FIG. 3-3 PRESSURE SOURCE SYSTEM

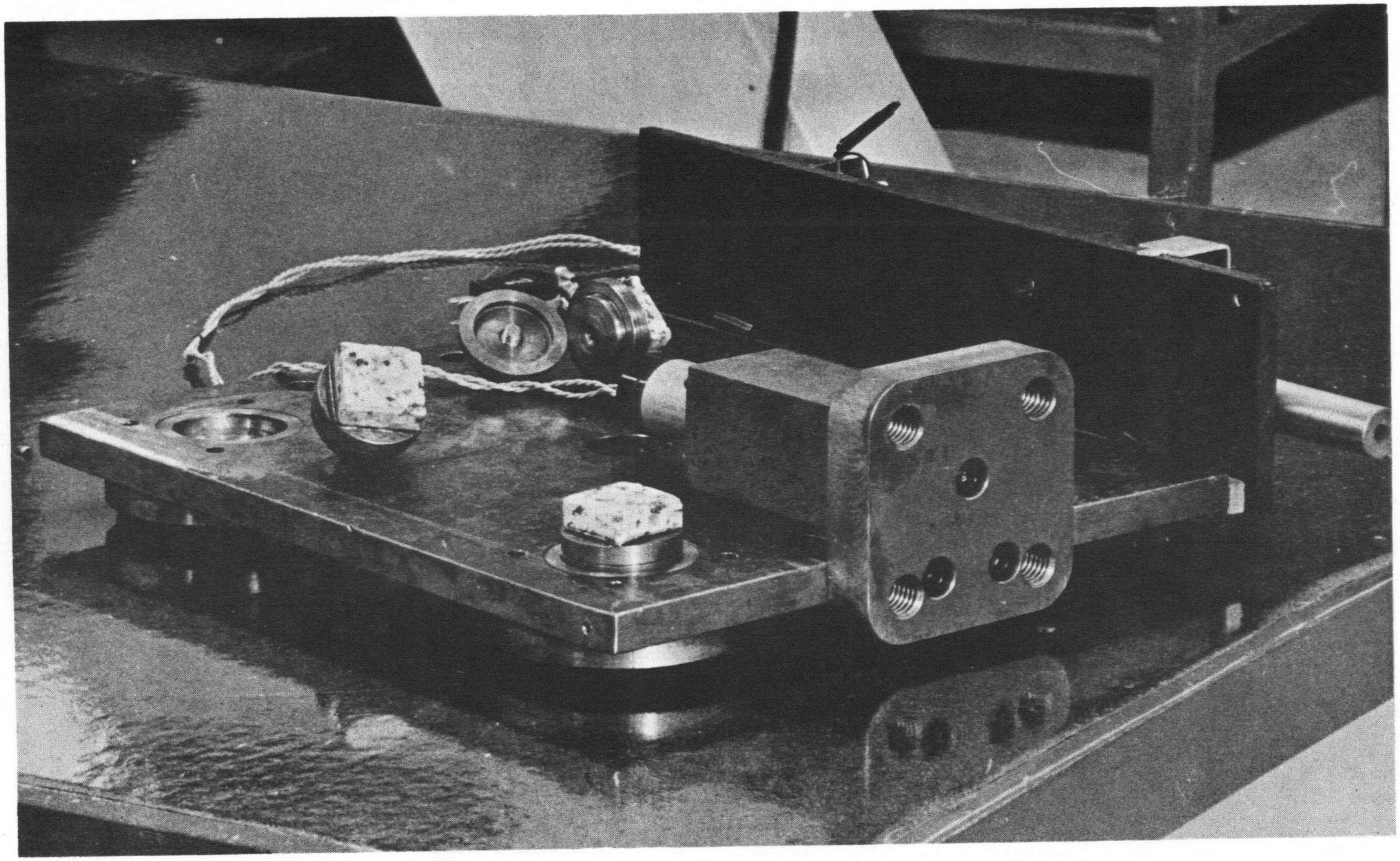

FIG. 3-4 CONFIGURATION OF THE PLATFORM AND THE SUSPENSION DEVICE

having a stiffness of 1.94 X 10^4 pounds per inch. A weight platen weighing 23.5 pounds was screwed to the top of the platform. It consisted of a circular disc and an upright post with its center line passing through the center of the platform so that the normal load was distributed equally on both sides thereby giving equalization of the frictional forces arising from each rail. This eliminated the moment, formed by unbalanced forces, that would tend to drive the platform toward on side. Nine circular lead weights with central holes had a total weight of 380 pounds could be placed on the load platen.

3-2. INSTRUMENTATION:

The friction force acting on the rubbing surfaces was measured by a strain-ring which had a stiffness of 1.94 X 10^4 pounds per inch. The strain-ring was mounted directly between the hydraulic ram and the platform so that the force acting on the platform could be measured. Four, 120 ohm strain gauges were mounted on the strain-ring. The gauges were connected to form a Wheatstone bridge as shown in Fig. 3-5. A bridge amplifier was connected to the bridge circuit so that any variation of the resistance of the gauges could be monitored. In previous work, a storage oscilloscope was used to display the friction force. However, an oscillograph with paper chart recording was found to be a better instrument to give permanent records. A Brush Model BL-932 D.C. Amplifier was matched to a Brush double trace

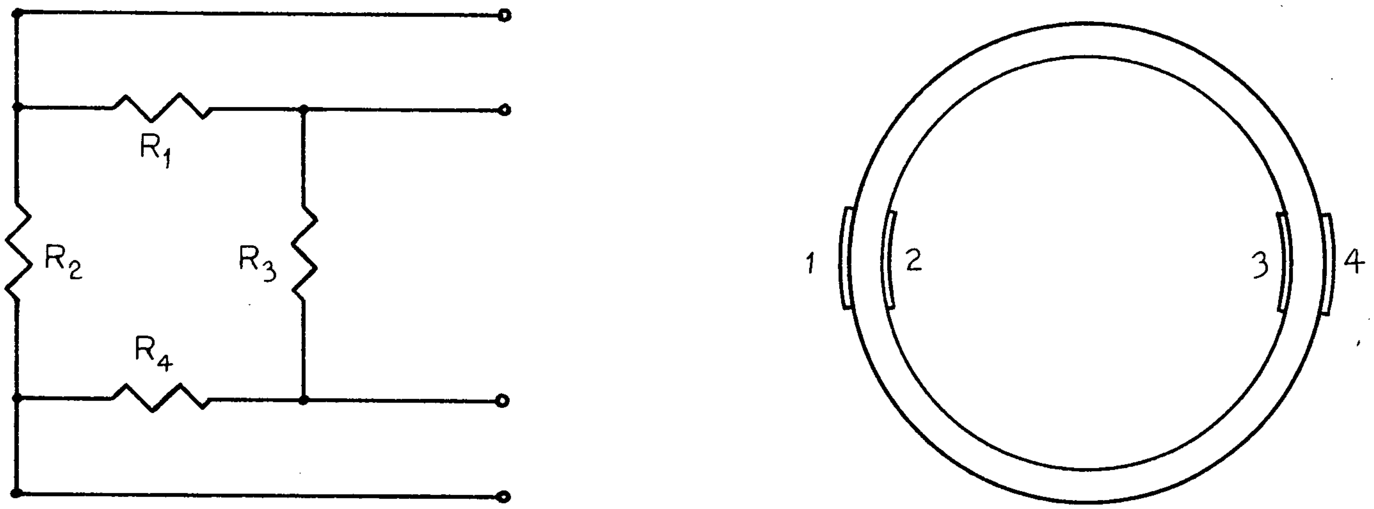

FIG. 3-5 WHEATSTONE BRIDGE CIRCUIT OF THE STRAIN RING

ultralinear oscillograph so that the output voltage of the bridge amplifier could be amplified sufficiently to drive the pen of the oscillograph. It was possible to record forces to an accuracy of 0.13 pounds per chart division. When compared with the nominal normal load of 50 pounds, the error of the measurement was considered to be acceptable.

The velocity of the sliding platform was monitored by a Sanborn LVsyn velocity transducer model 6-LV-4, which was design as a magnet bar moving through an induction coil such that a voltage was induced with a magnitude linearly proportional to the velocity of the moving magnet. The usable stroke of this transducer was four inches. It was long enough to cover more than one thousand stick-slips since the amplitude of stick-slip vibration was of the order of 4×10^{-4} inches for pyrite and 4×10^{-3} inches for glass.

Consider equation (2-5) in chapter two:

$$M\ddot{x} + C\dot{x} + Kx = W\mu \qquad (3-1)$$

In a very lightly damped system C is negligible and the equation reduces to

$$M\ddot{x} + Kx = W\mu$$

or

$$\frac{M}{W}\ddot{x} + \frac{K}{W}x = \mu \qquad (3-2)$$

Equation (3-2) shows that, with a suitable choice of scales for $\ddot{x}$ and x, μ can be obtained by the vector sum of the signals $\ddot{x}$ and x (16, 34). The coefficient of kinetic friction, μ_m, values of the present experiment were obtained in the μ-V curves recorded during slip.

A Kistler servo accelerometer with a sensitivity of 0.1 volt per unit gravity was used in the combination with the displacement transducer and the velocity transducer from which the μ-V relationship at slip could be displayed on an oscilloscope.

3-3. SPECIMENS AND PREPARATION OF SLIDING SURFACES:

Four types of rock were used in the tests. These specimens were prepared and finished with a diamond saw and geological polishing equipment. Pyrite, a mineral of iron disulphide, exists in the form of octahedral and cubic crystals in metamorphic rocks, with a shear modulus of 0.7 X 10^6 bars (36). Green schist, a chlorite schist, is composed of various minerals, such as magnetite and garnet, in a form of non-homogeneous fabric-like crystals. The mechanical properties of green schist, with a shear modulus of 0.315 X 10^6 bars (36), are affected by the orientation of the crystals. In addition, green schist splits very easily. The third rock specimen was obtained from the Hope slide in British Columbia at Mile on the Hope-Princeton Highway. It has been classified as a black marble. Black marble, a hard metamorphic limestone, has a homogeneous structure with a shear modulus of 0.229 X 10^6 bars (36). Granodiorite, a coarse granular intrusive igneous rock, has its constitution between that of granite and quartz-diorite. Its shear modulus is 0.25 X 10^6 bars (36). In addition to the rock materials, steel and glass were also tested. The steel results provided a tie with earlier experimental results of other workers. Glass, on the other hand, is a material similar to some rocks and possesses a homogeneous structure.

Three sliders were used in each test. Pyrite and black marble sliders were cut to 1.25 inch squares with a thickness of 0.5 inch. The green schist sliders were cut in 0.75 inch squares with a thickness of 0.4 inch. Granodiorite and glass sliders were cut in one inch squares with thicknesses of 0.375 and 0.25 inches respectively. The length of the rails varied according to the available size of rock before cutting. However, a running distance of 4 inches could be obtained for all rocks and lengths of more than 12 inches were easily obtained for glass and steel. Epoxy was used to glue the sliders onto slider adapters. The rails and sliders are shown in Fig. 3-6.

After cutting the surfaces of the rock specimens were carefully ground to an average finishes as shown below, and were washed thoroughly with distilled water in order to remove grinding contaminant.

	SURFACE FINISH C. L. A. (micro inches)
PYRITE	90
BLACK MARBLE	60
GREEN SCHIST	220
GRANODIORITE	53

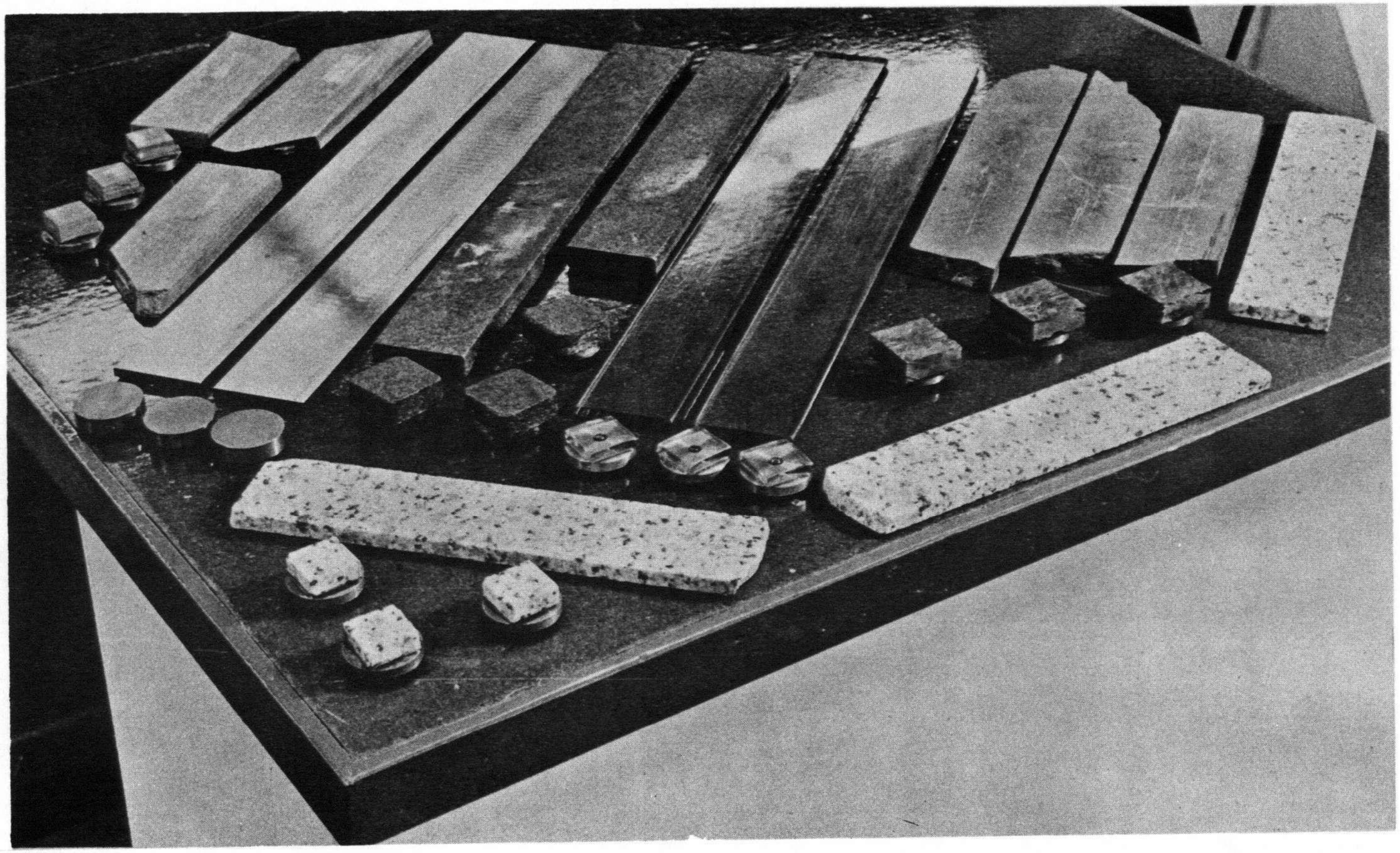

FIG. 3-6 SPECIMENS
A. GREEN SCHIST, B. 1020 STEEL, C. PYRITE,
D. GLASS, E. BLACK MARBLE, F. GRANODIORITE.

CHAPTER IV

EXPERIMENTAL RESULTS

4-1. PROCEDURE:

The general preparation of the test specimens has been described in chapter three. However, all specimens received additional treatment immediately before test as follows:

(a) Steel sliders and rails were washed by trichloro-ethylene and alcohol. A layer of lubricant, the same as was used in the test, was immediately coated on the newly washed surfaces in order to limit atmospheric contamination.

(b) Rock specimens were washed with distilled water. Tap water was not used in order to avoid minerals that would adhere to the surfaces and affect the frictional results. The specimens were then heated in an oven at $100^{\circ}C$ for one and half hours so that moisture was evaporated away from the specimens, they were then cooled to room temperature before they were put to test.

(c) Glass was cleaned with trichloro-ethylene in order to remove the grease on the surfaces. The specimens were then washed with alcohol and distilled water, and dried at room condition.

Three sliders were placed on two parallel rails which were clamped on a lathe bed. Lubricant, if needed, was spread on the rails and was coated evenly by moving the sliders over the rails. The platform was placed on the sliders and connected to a strain-ring which was fixed at the end of the piston rod of the hydraulic cylinder. Lead weights were put on the weight-carrier over the platform. Normal load could be varied from 50 pounds to 430 pounds in increments of about 40 pounds.

With the valves closed the oil pressure was raised to 1000 psi and with the pump still running the valves were turned on and the slider platform was driven at high speed. More than two hundred strokes were made on steel before the first set of data was taken; about twenty strokes were made on rocks, at a fairly low speed; and no run-in procedure was used for glass.

In the tests, the driving speed was set at a high value, then reduced gradually until the hydraulic fluid ceased to flow, thereby giving driving speeds ranging from zero to two inches per second.

In the vibrational system, both the stiffness, K and the damping coefficient, C were constant; the only variables considered were $\dot{\theta}$ and normal load. These restrictions were related to the structure of the apparatus whereby it was not possible to vary K and C without disassembling the system.

The diameter or the length of the sliders were 0.75 inch to 1.25 inches. One inch of displacement of the sliders would be accomplished in about two hundred stick-slip cycles. A reasonable consistency of the surface condition existed over such a short distance.

4-2. RESULTS:

For the purposes of explaining the mechanism of earthquakes, coefficient of friction versus $\log_{10} \dot{\theta}$ curves and amplitude of vibration versus $\log_{10} \dot{\theta}$ curves were intensively considered.

Lubricated and unlubricated tests were conducted. Water was used as lubricant for all specimens although petrolatum oil was used on pyrite and glass after sufficient data using water had been obtained.

4-2-1. 1020 STEEL:

Steel was tested under four different conditions; namely, heavy petrolatum (H.P.) as lubricant, light petrolatum (L.P.) as lubricant, water and dry conditions. Figs. 4-1, and 4-2 display the results with the H.P. lubricant. The results of steel with light petrolatum gave no significant difference from that of steel with H.P. Figs. 4-3 and 4-4 are the results of water on steel, Figs. 4-5 and 4-6 are the μ and α curves for dry steel, and the results are almost the same as water on steel.

4-2-2. GLASS:

Three conditions were considered in the tests of glass. Figs. 4-7 and 4-8 are the results for dry glass, and Figs. 4-9 and 4-10 show the results for wet glass. Figs. 4-11 and 4-12 are the results of glass with L.P.

Water gave no obvious change in the maximum friction but increased the amplitude by an order of five. A layer of mineral oil gave an obvious drop of μ_{max}, from 0.9 to 0.4, and μ_{min}, from 0.65 to 0.15.

4-2-3. PYRITE:

Figs. 4-13 through to 4-18 are the static friction and amplitude results of pyrite under dry, wet and lubricated conditions. The addition of water lowered μ_{max} from 0.32 to 0.22 and the amplitude to 50% of that of dry pyrite.

4-2-4. BLACK MARBLE:

Two conditions were examined for this material. Figs. 4-19 and 4-20 show the friction and amplitude curves water was used as the lubricant. Relatively high friction values were found. The friction of the dry marble was investigated but very scattered results were obtained.

4-2-5. GREEN SCHIST:

Several tests were conducted with green schist, but no friction induced vibration was observed. It was believed that the difference between μ_s and μ_m of green schist was so small that the amplitude of stick-slip vibration could not be measured. The average coefficients of friction of dry and wet green schist were 0.66 and 0.58 respectively.

4-2-6. GRANODIORITE:

Granodiorite was the only igneous rock used in the experiments. The frictional behaviour of granodiorite was very similar to that of black marble. Dry granodiorite gave no stick-slip vibration, but gave a fairly constant coefficient of friction of about 0.72. The friction versus $\log_{10} \dot{\theta}$ and amplitude versus $\log_{10} \dot{\theta}$ curves of wet granodiorite are shown in Figs. 4-21 and 4-22 respectively. The maximum coefficient of friction was 0.65 and the kinetic coefficient of friction was 0.55.

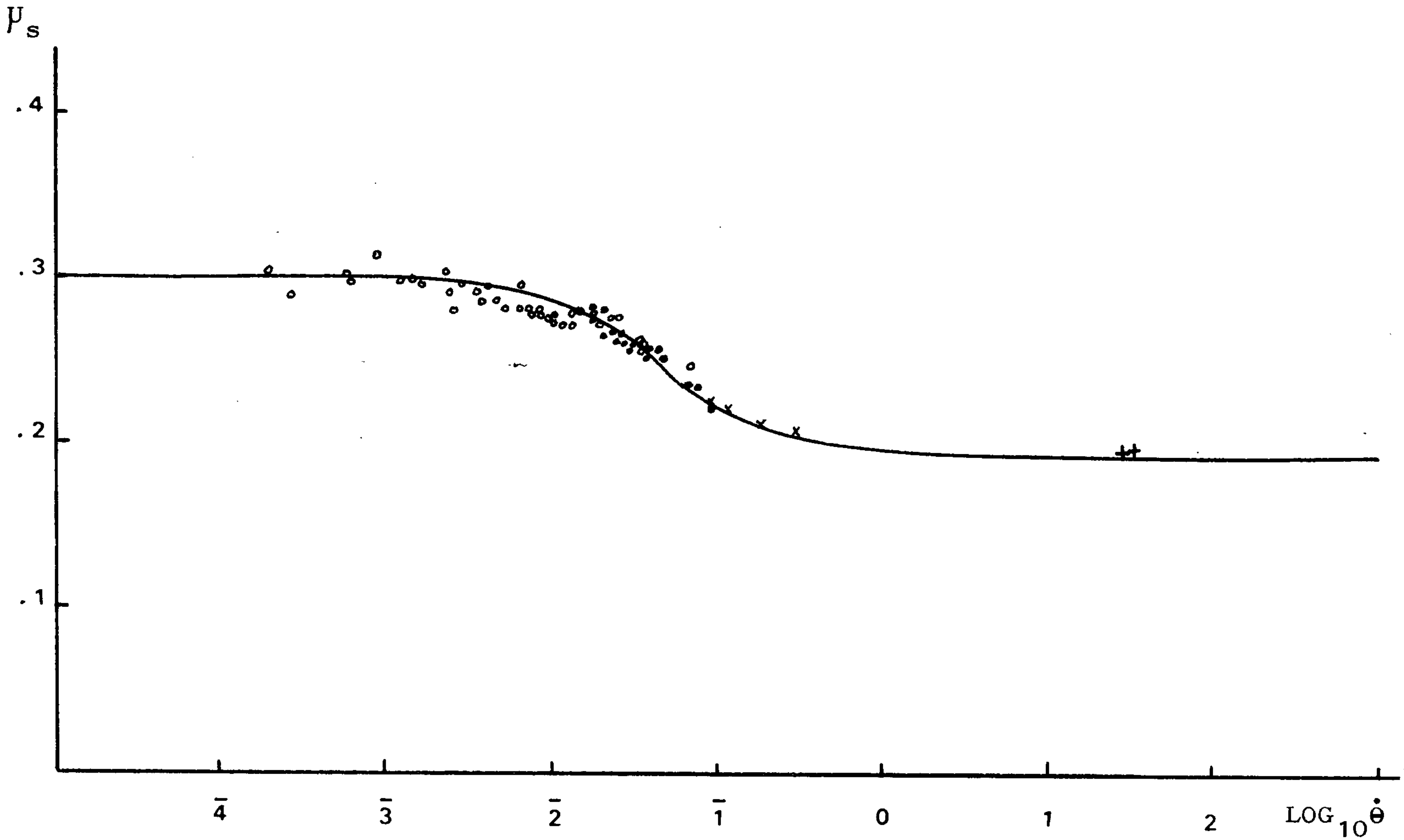

FIG. 4-1 μ_s VERSUS $\mathrm{LOG}_{10}\dot{\theta}$ —— STEEL WITH LUBRICANT (H.P.)

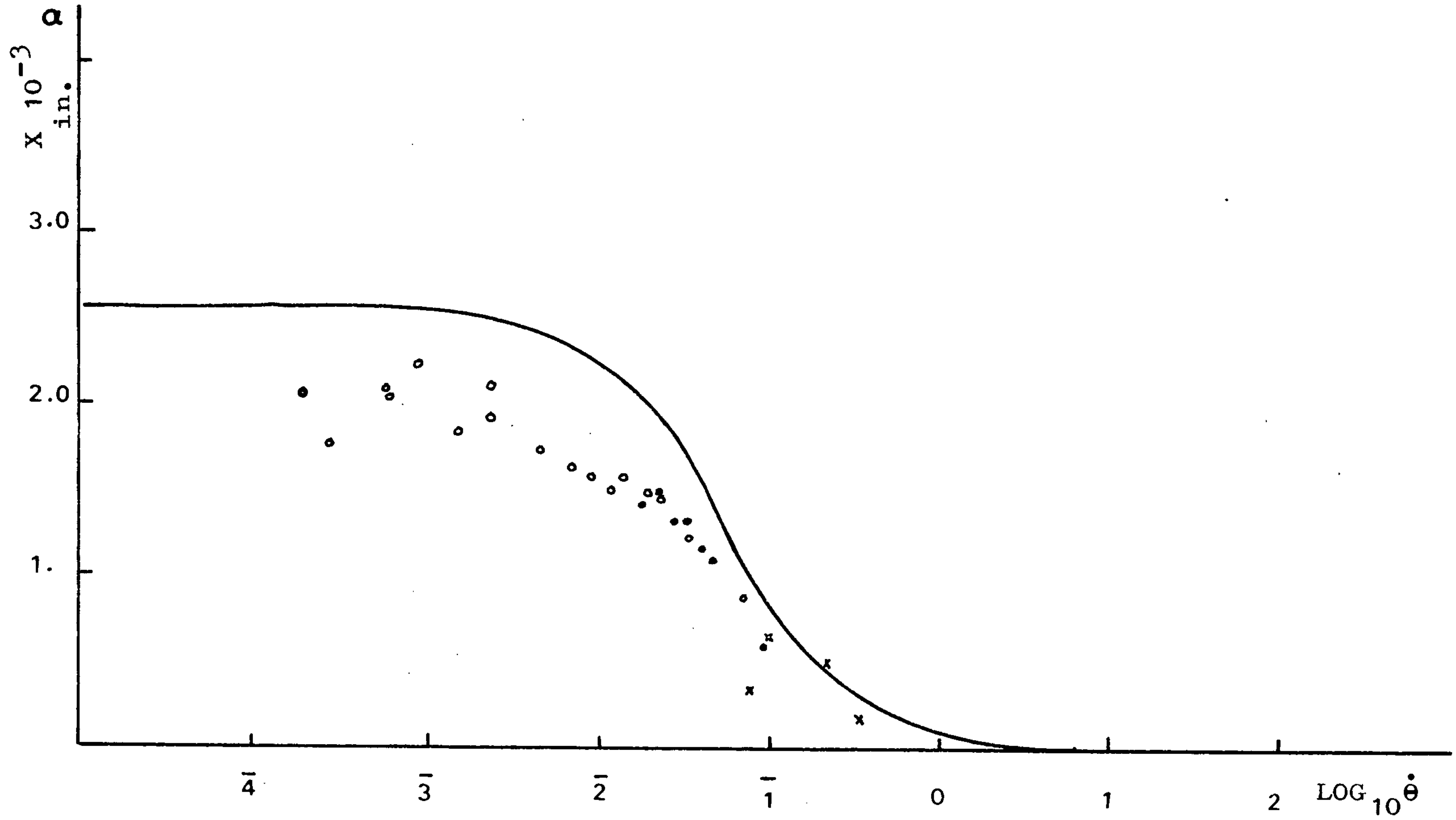

FIG. 4-2 α VERSUS $LOG_{10}\dot{\theta}$ — STEEL WITH LUBRICANT (H.P.)

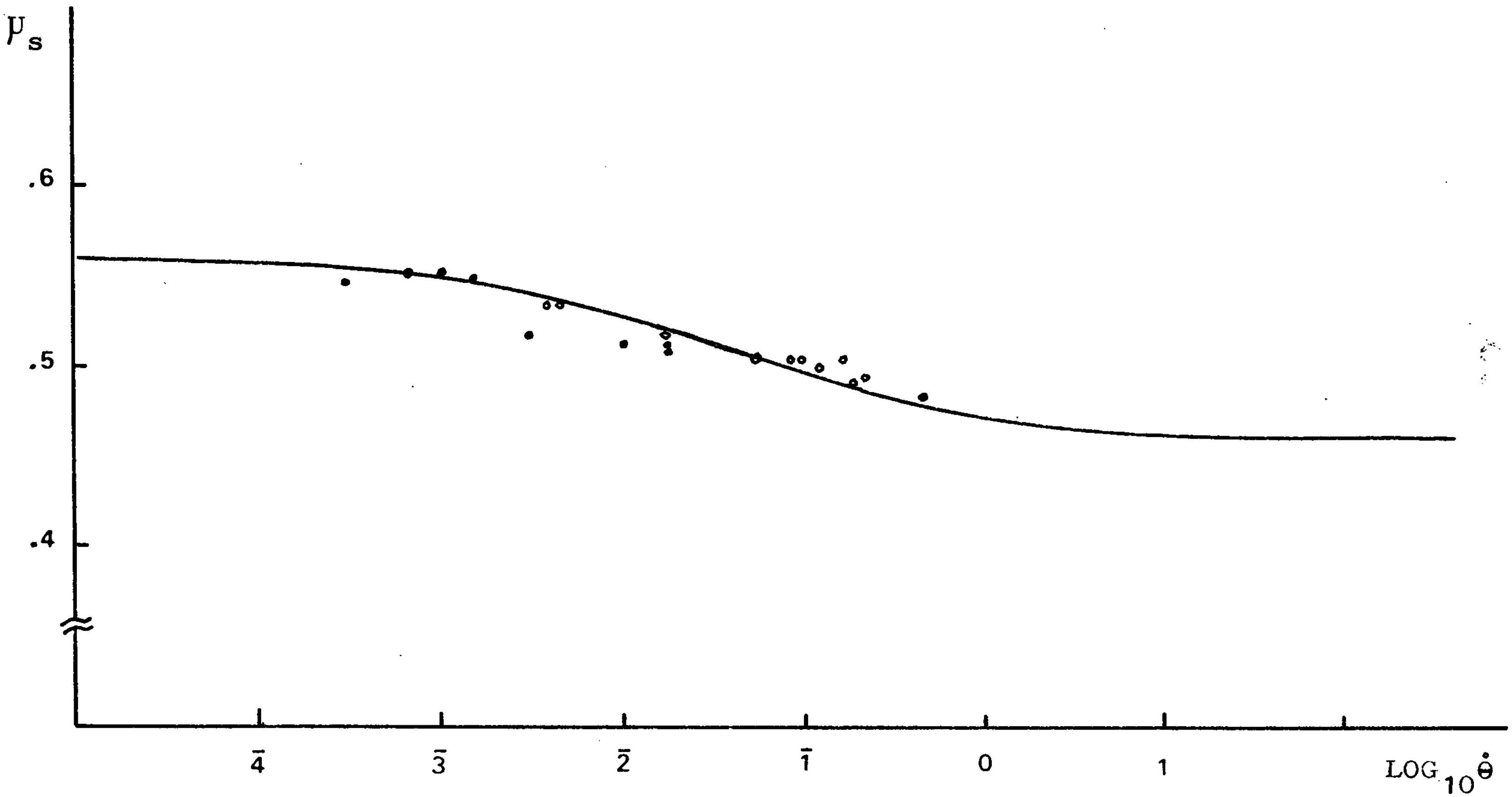

FIG. 4-3 μ_s VERSUS $LOG_{10}\dot{\theta}$ — WATER ON STEEL

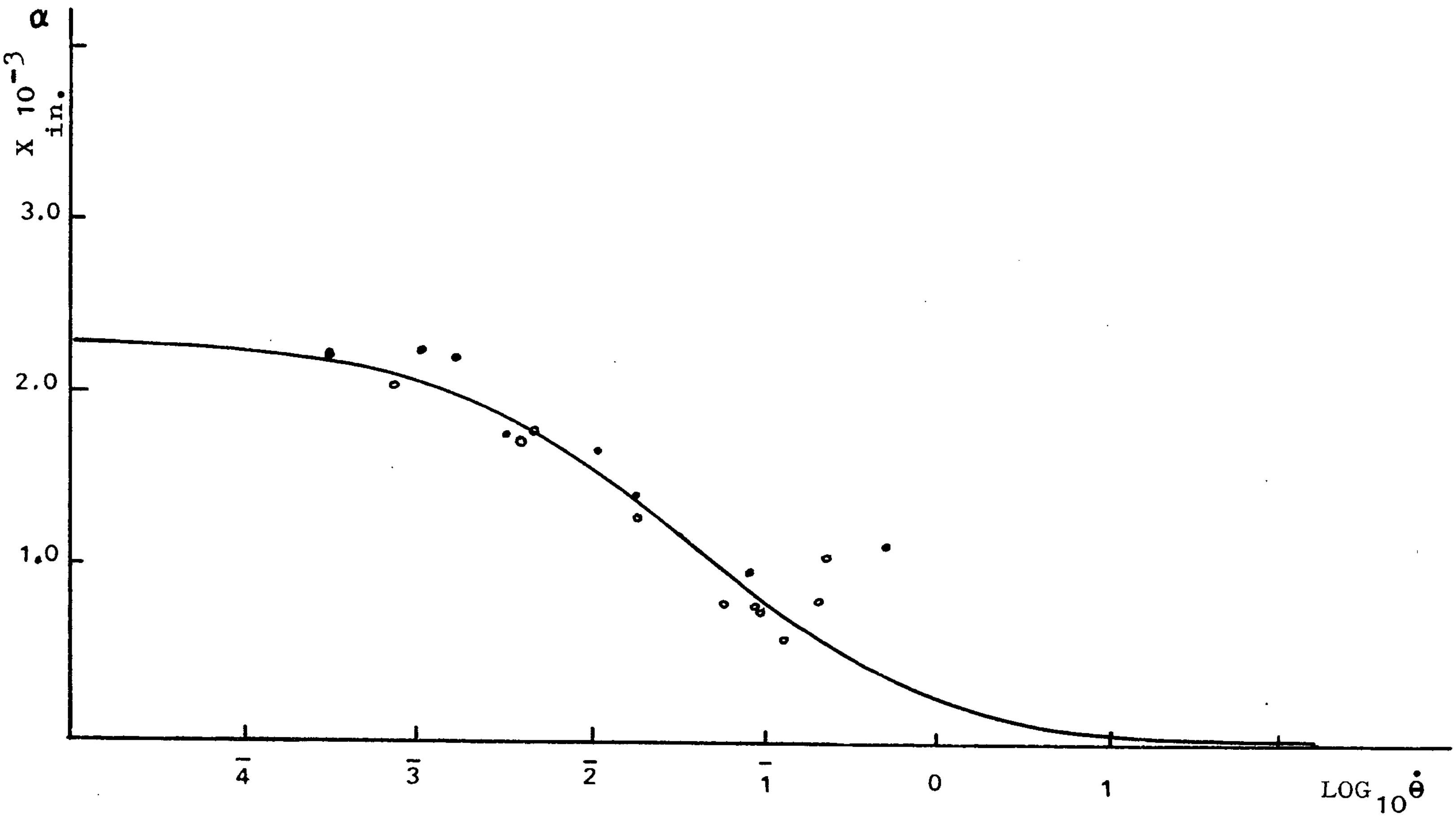

FIG. 4-4 α VERSUS LOG$_{10}\dot{\theta}$ — WATER ON STEEL

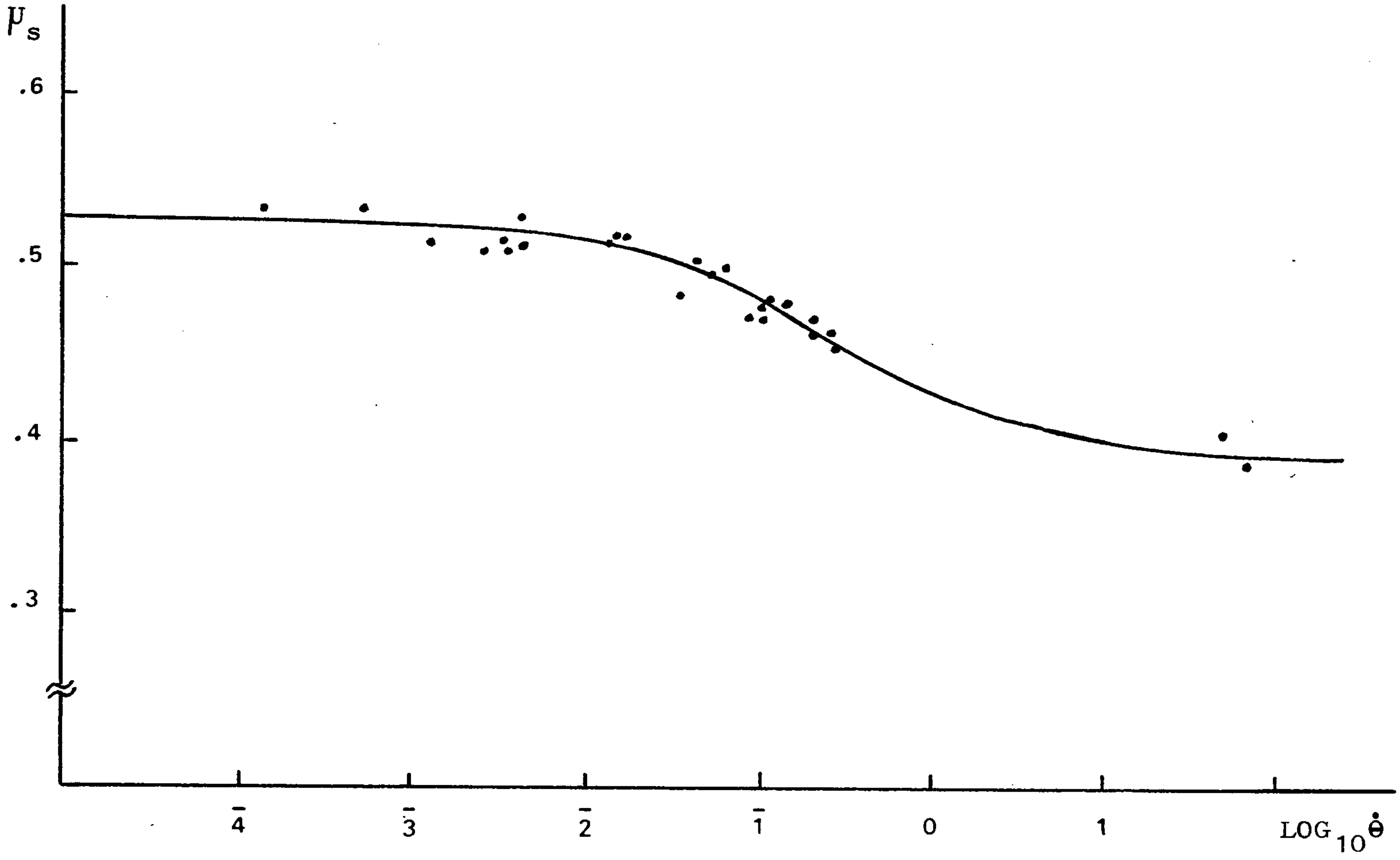

FIG. 4-5 μ_s VERSUS $LOG_{10}\dot{\theta}$ —— DRY STEEL

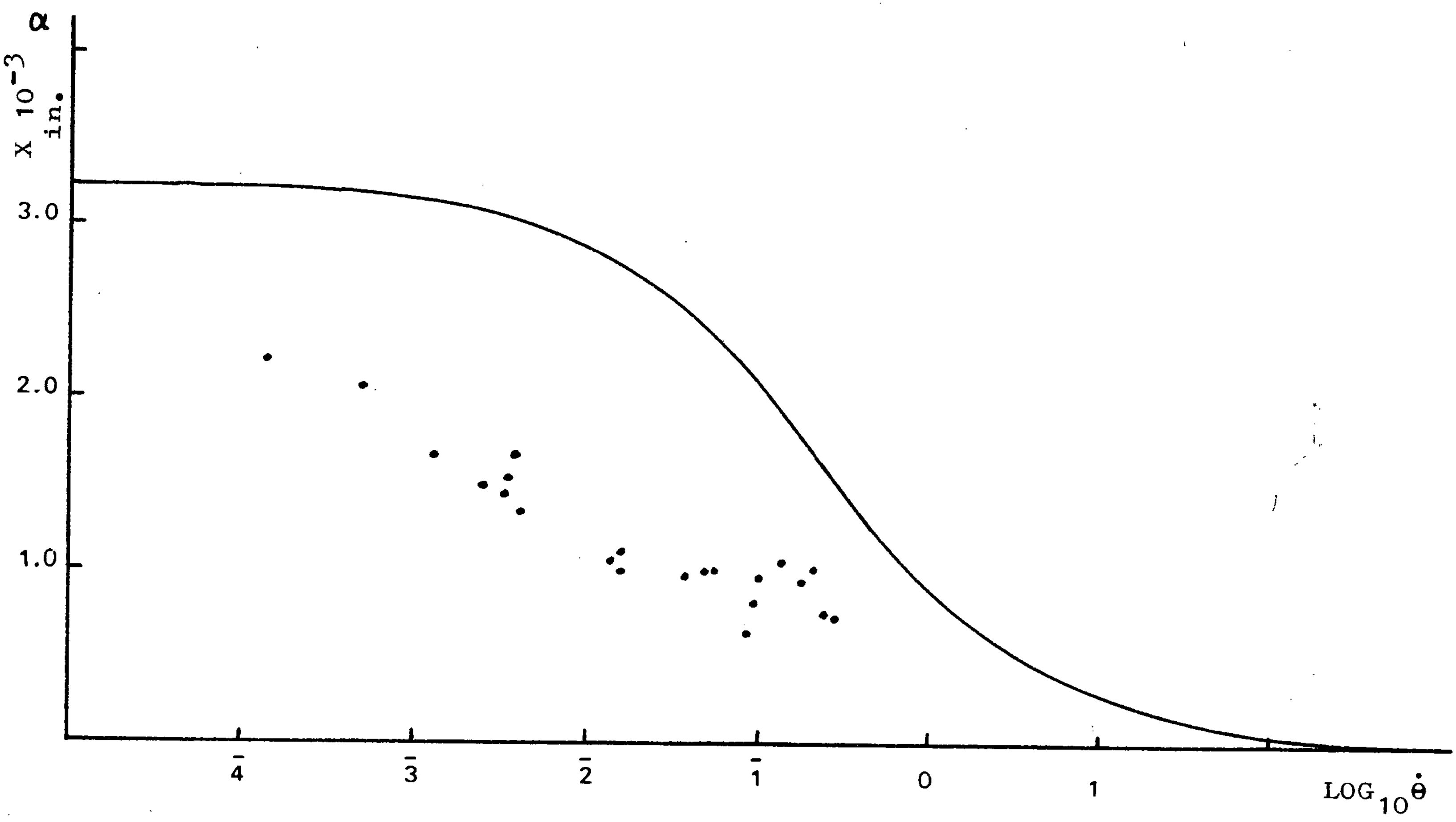

FIG. 4-6 α VERSUS $LOG_{10}\dot{\theta}$ —— DRY STEEL

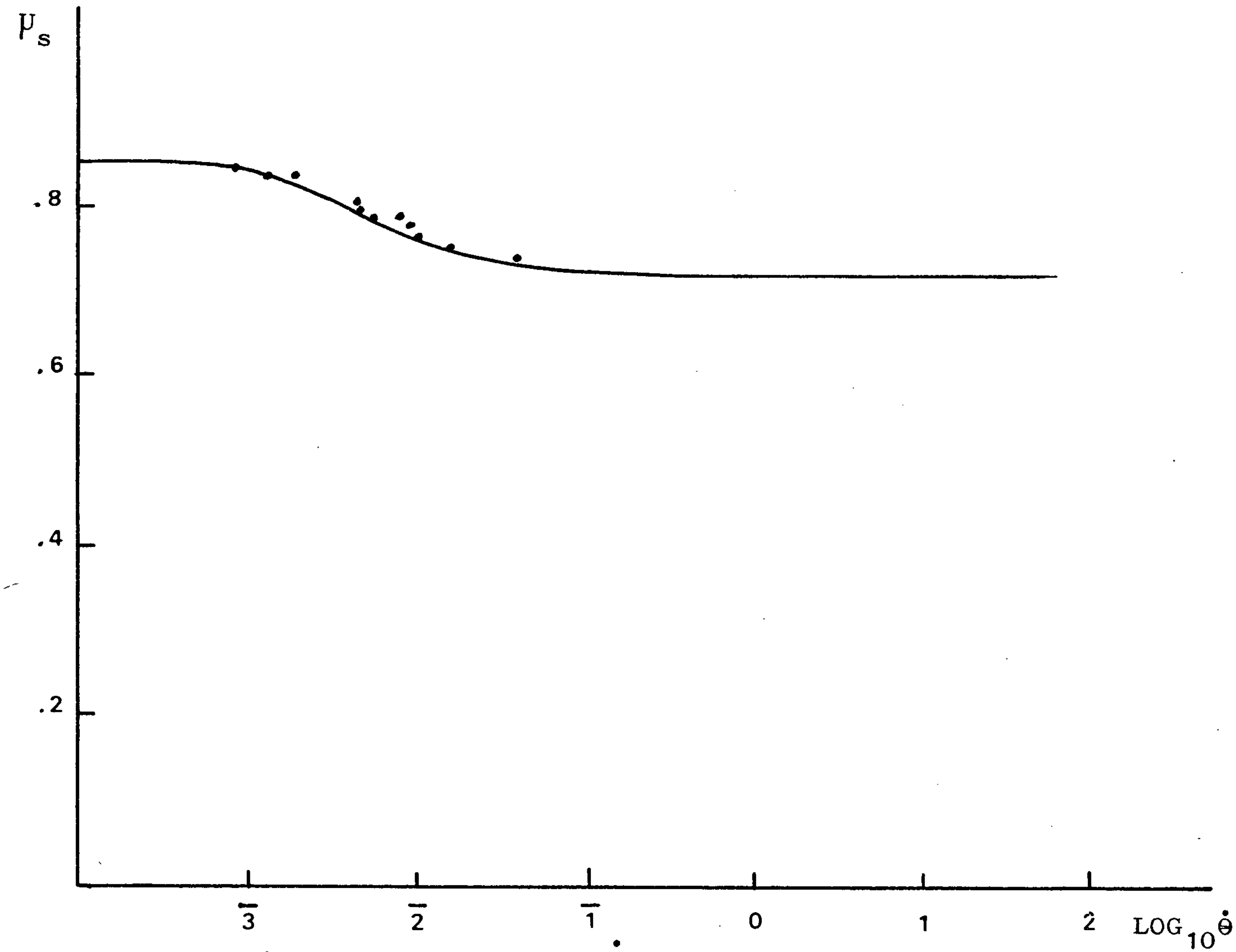

FIG. 4-7 μ_s VERSUS $LOG_{10}\dot{\theta}$ — DRY GLASS

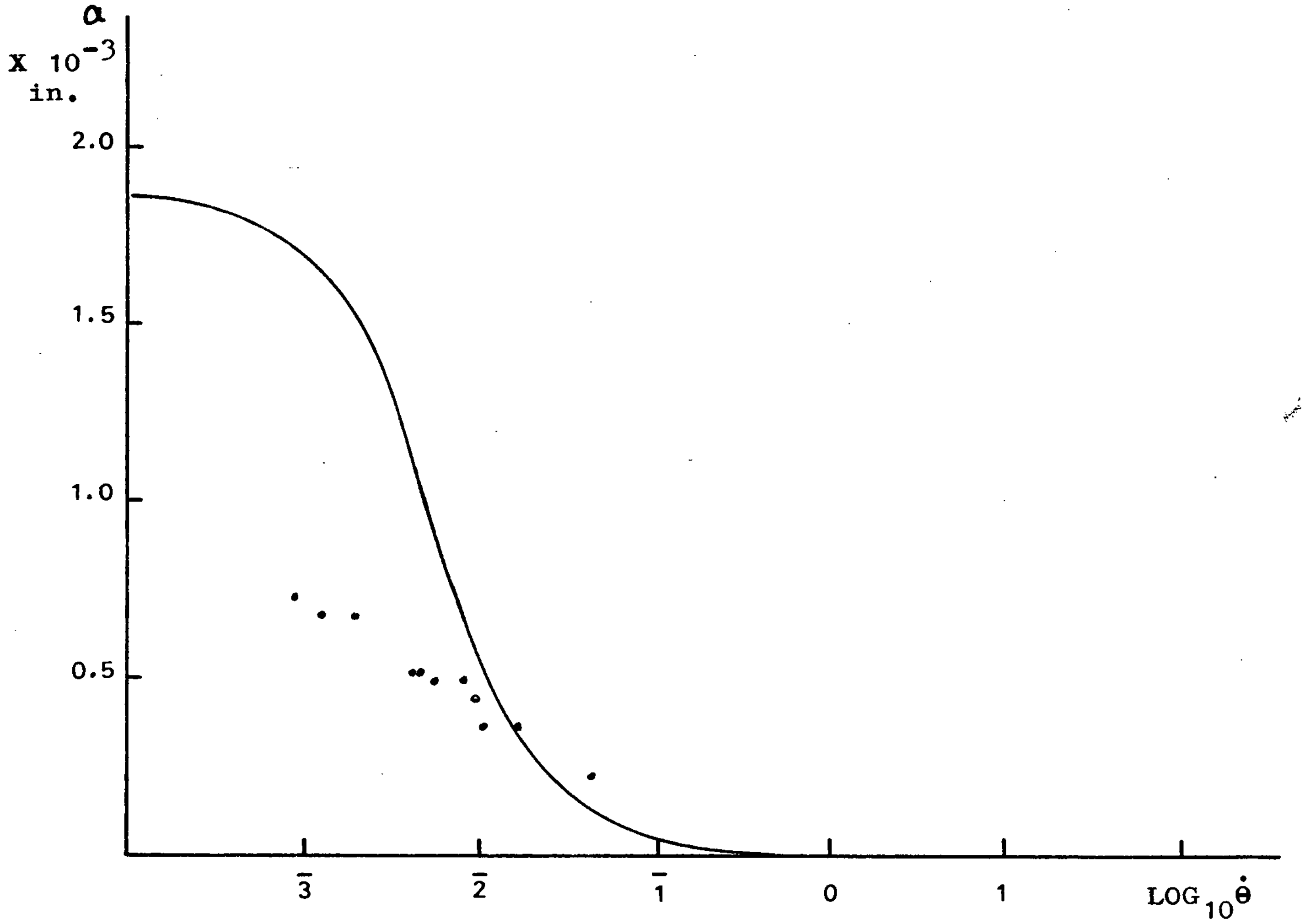

FIG. 4-8 α VERSUS $LOG_{10}\dot{\theta}$ —— DRY GLASS

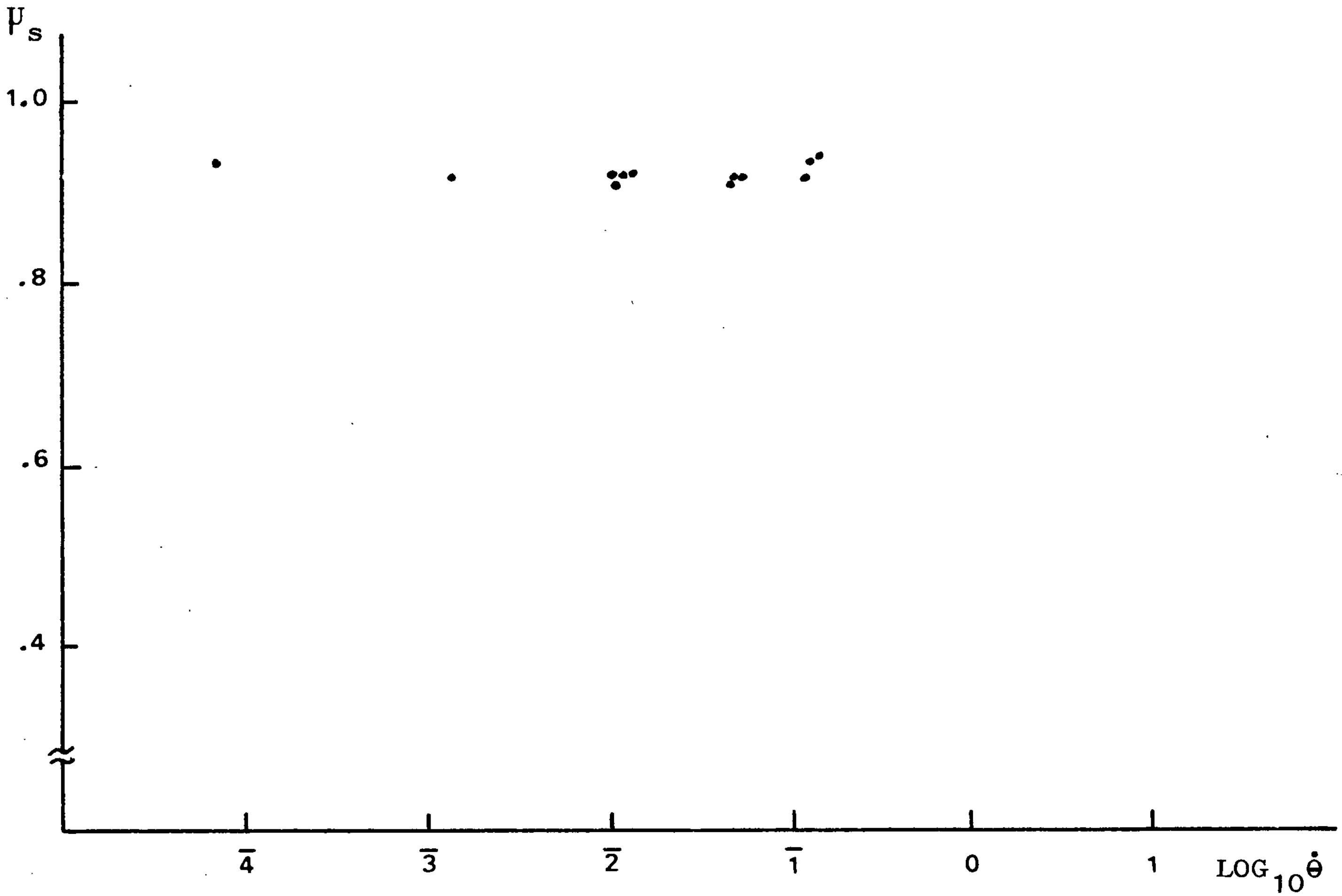

FIG. 4-9 μ_s VERSUS $LOG_{10}\dot{\theta}$ —— WET GLASS

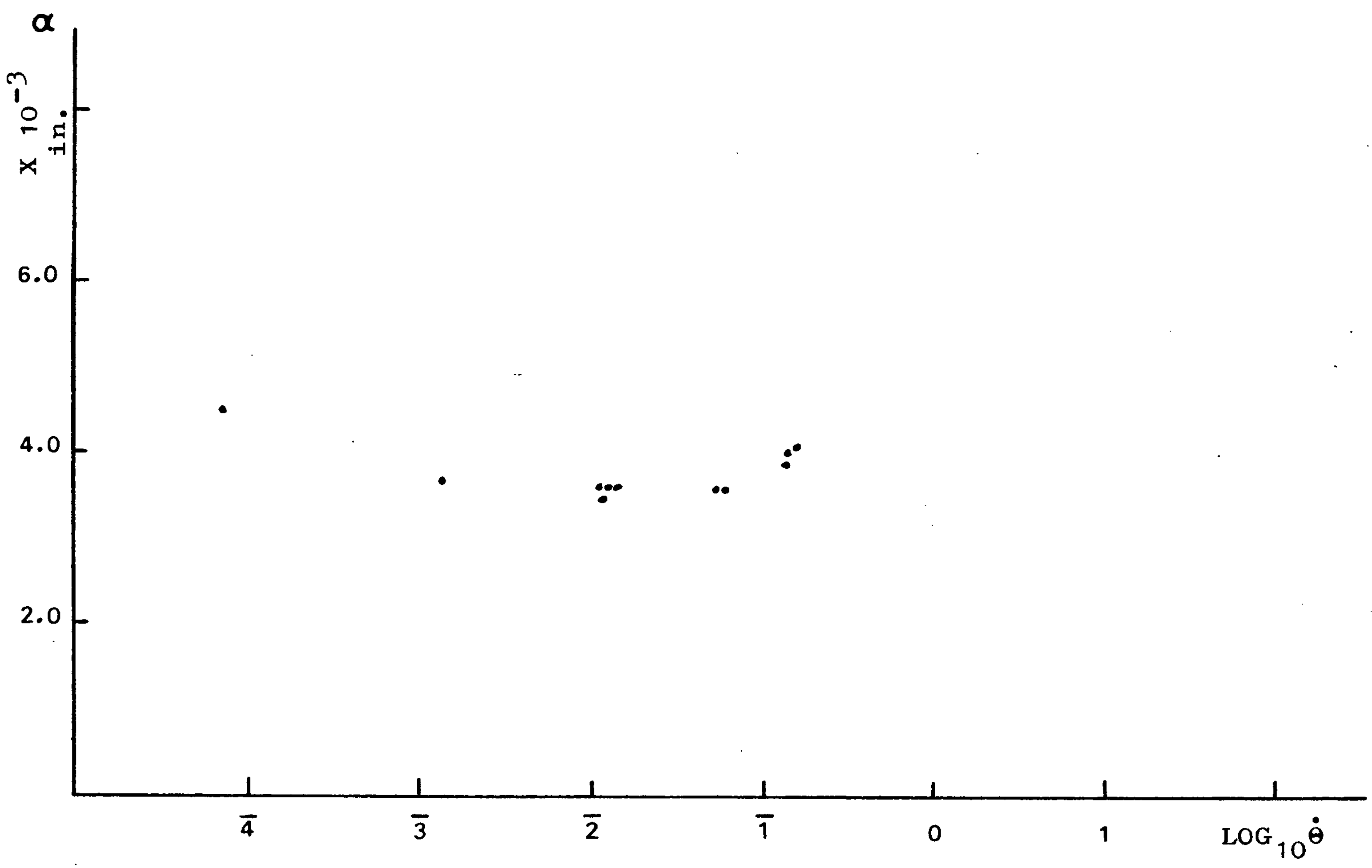

FIG. 4-10 α VERSUS $LOG_{10}\dot{\theta}$ —— WET GLASS

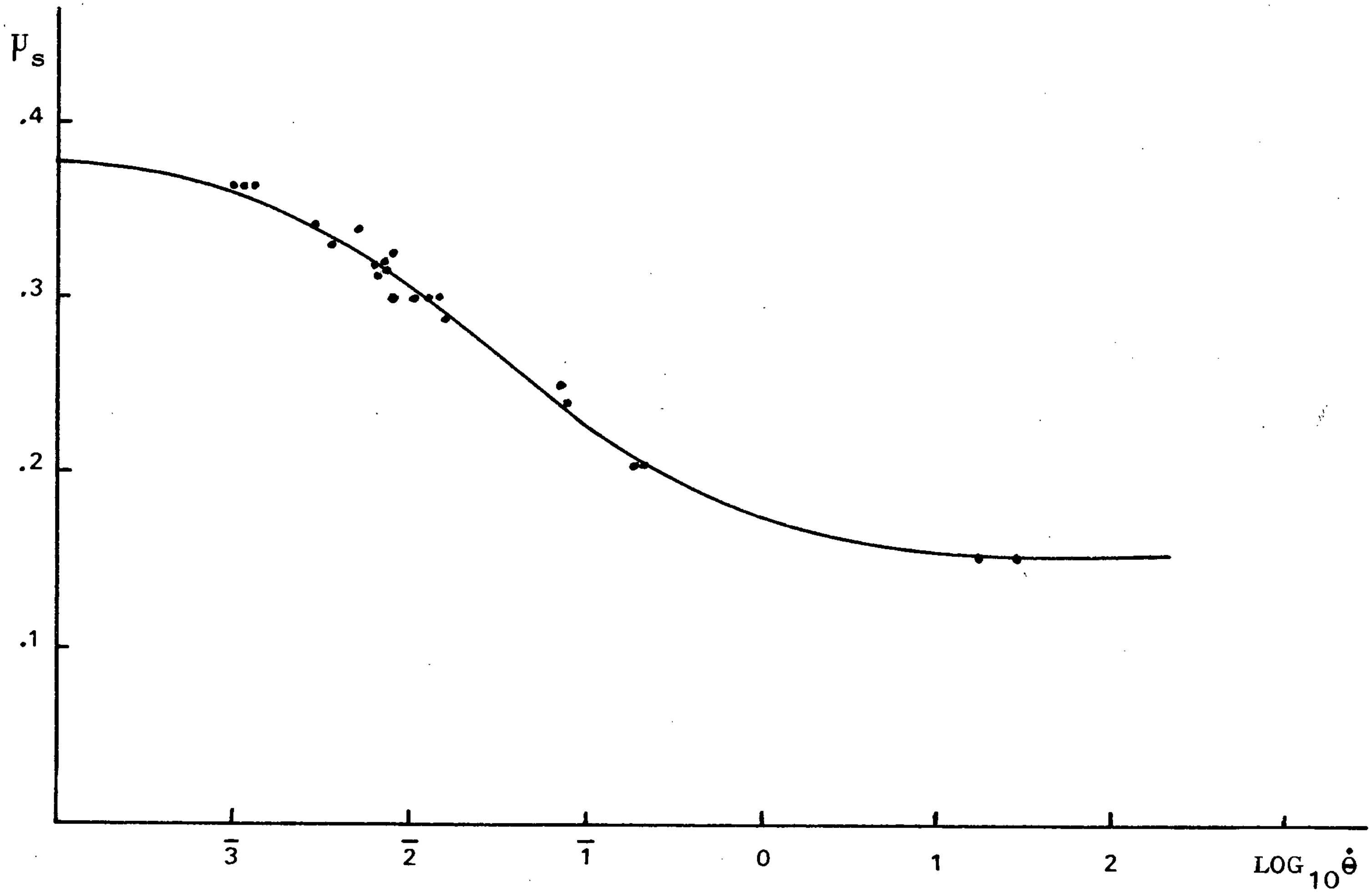

FIG. 4-11 μ_s VERSUS $\text{LOG}_{10}\dot{\theta}$ — GLASS WITH LUBRICANT (L.P.)

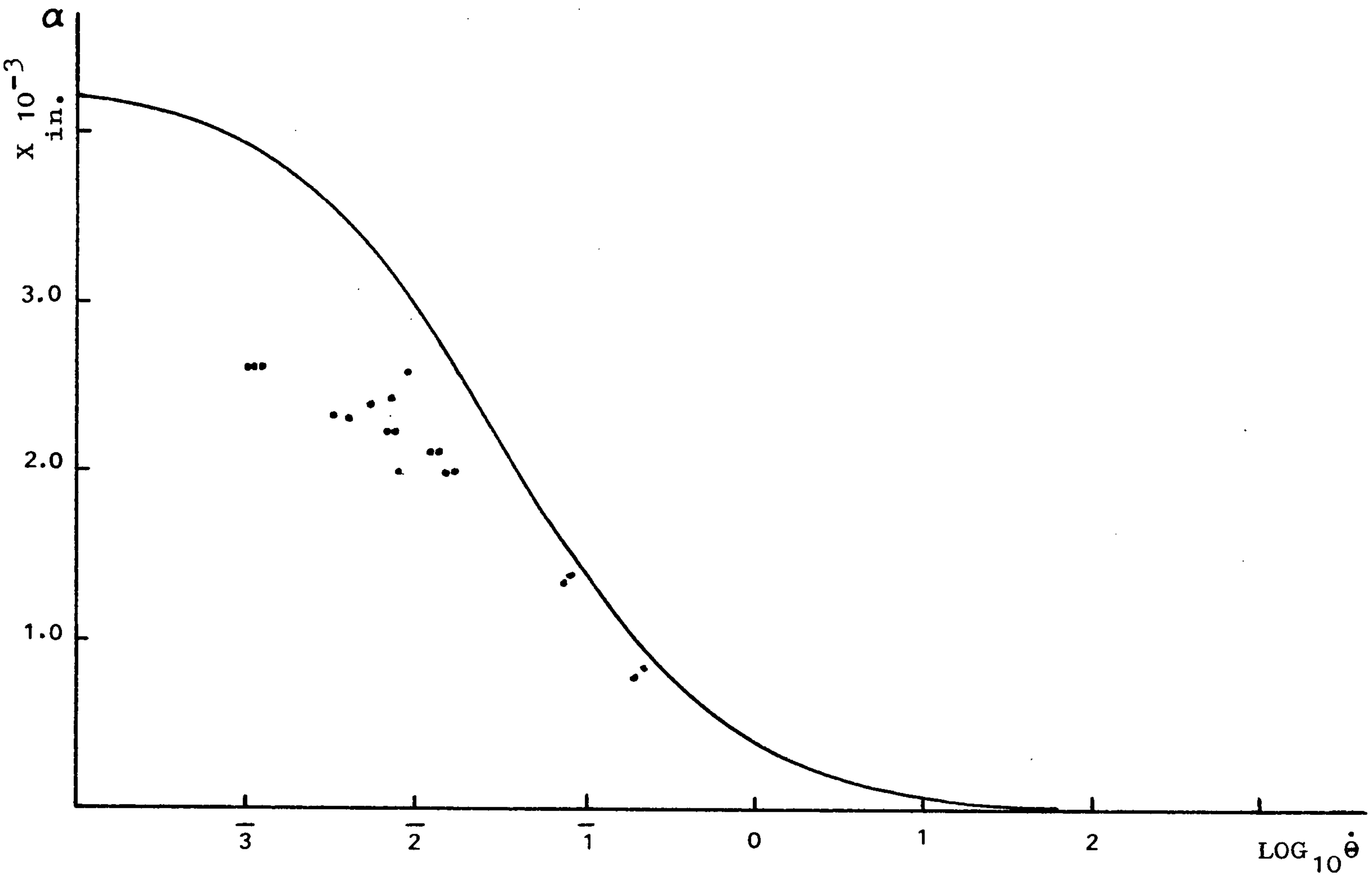

FIG. 4-12 α VERSUS $LOG_{10}\dot{\theta}$ —— GLASS WITH LUBRICANT (L.P.)

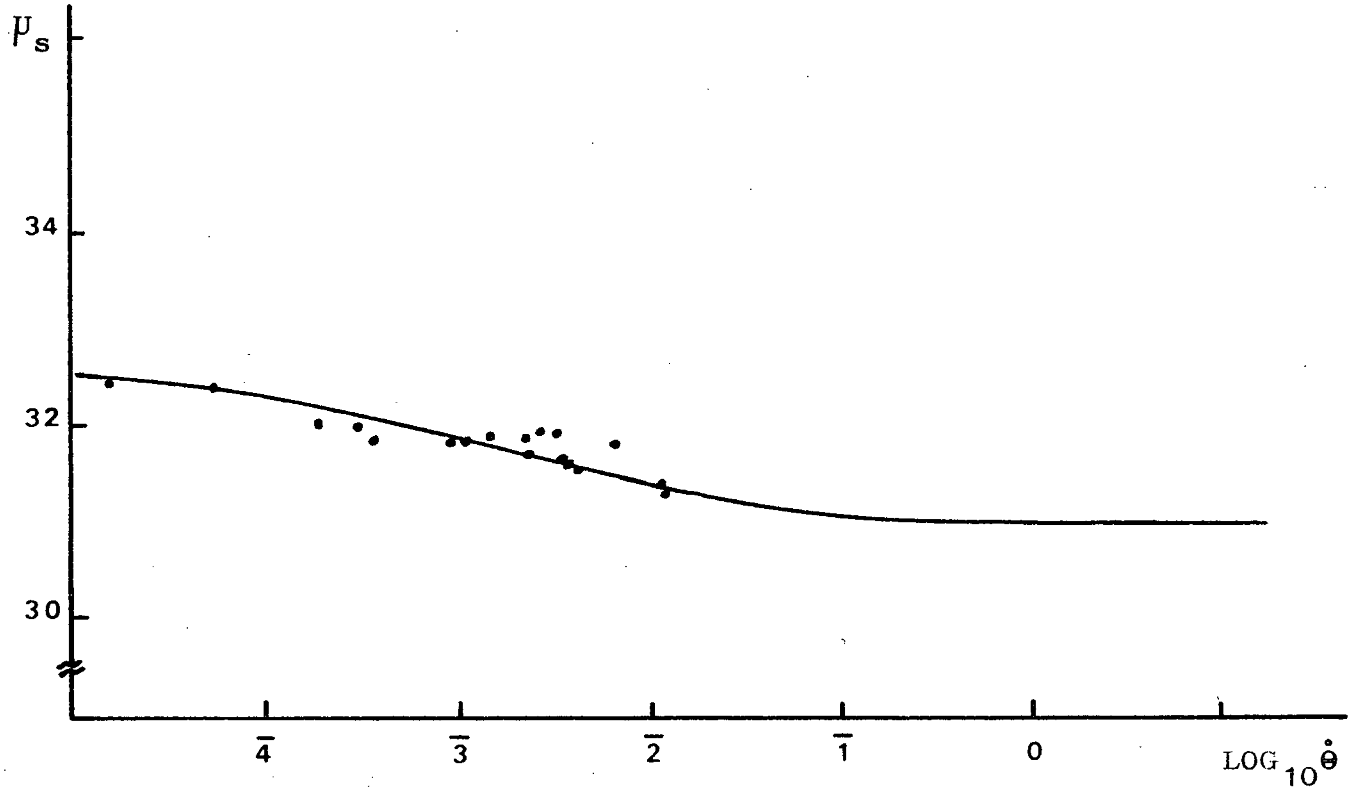

FIG. 4-13 μ_s VERSUS $LOG_{10}\dot{\theta}$ — DRY PYRITE

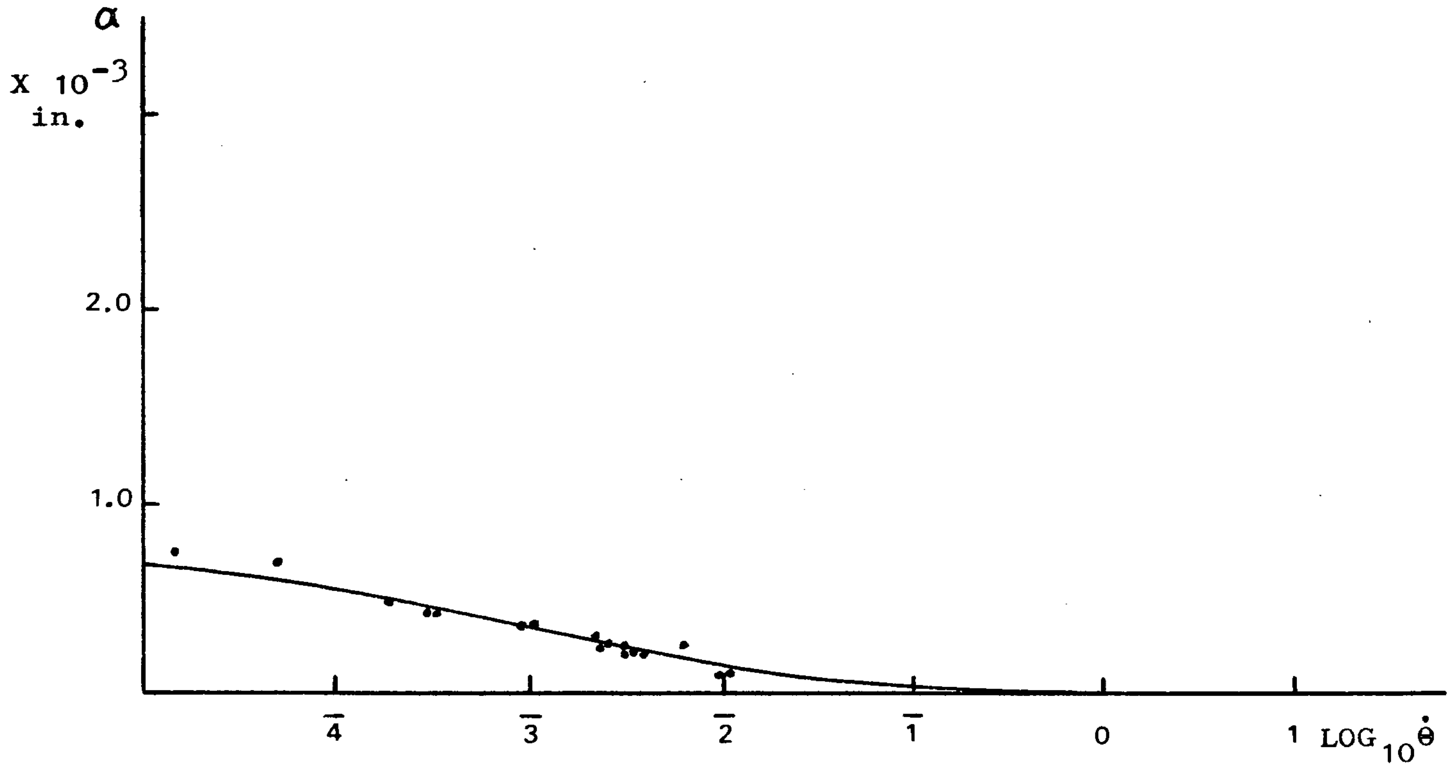

FIG. 4-14 α VERSUS $LOG_{10}\dot{\theta}$ —— DRY PYRITE

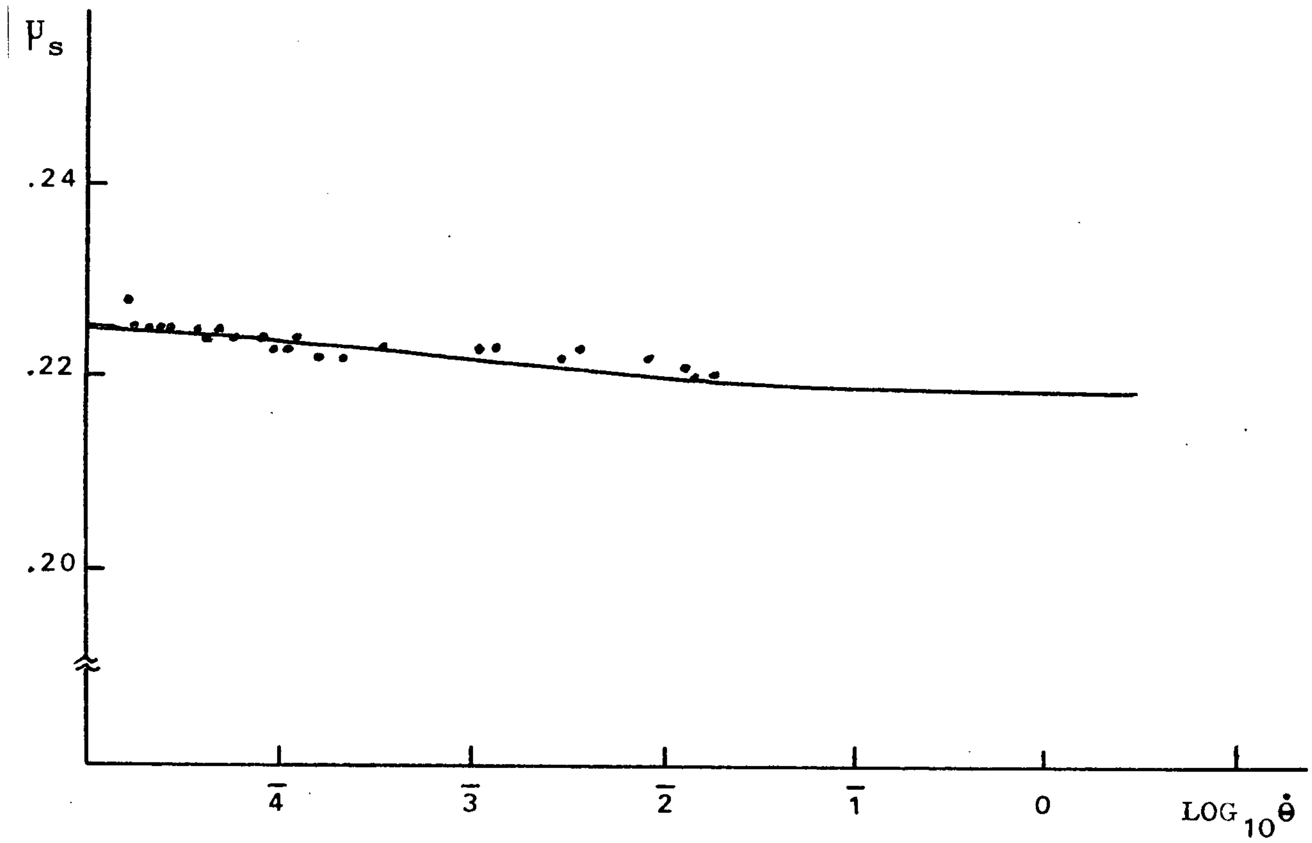

FIG. 4-15 μ_s VERSUS $LOG_{10}\dot{\theta}$ — WET PYRITE

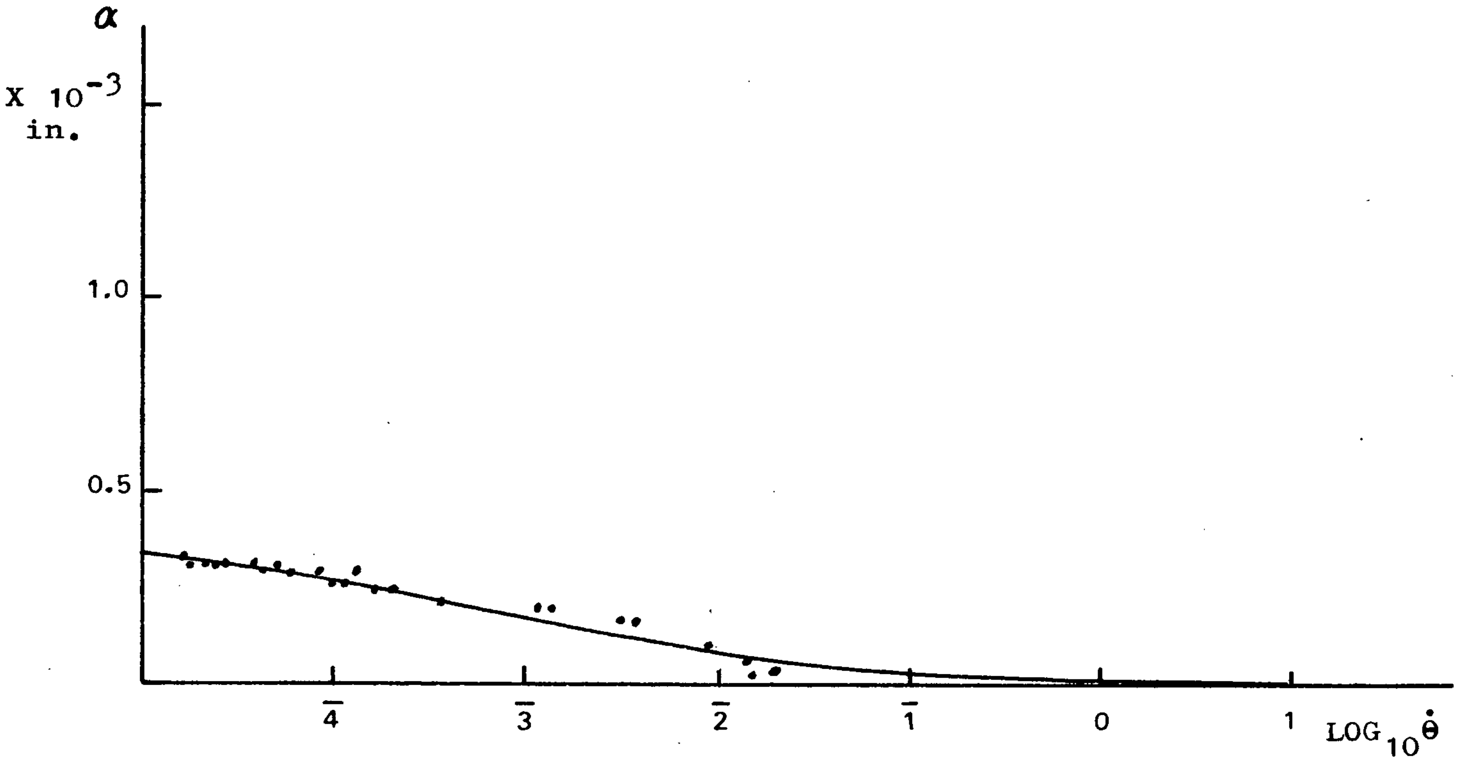

FIG. 4-16 α VERSUS $LOG_{10}\dot{\theta}$ —— WET PYRITE

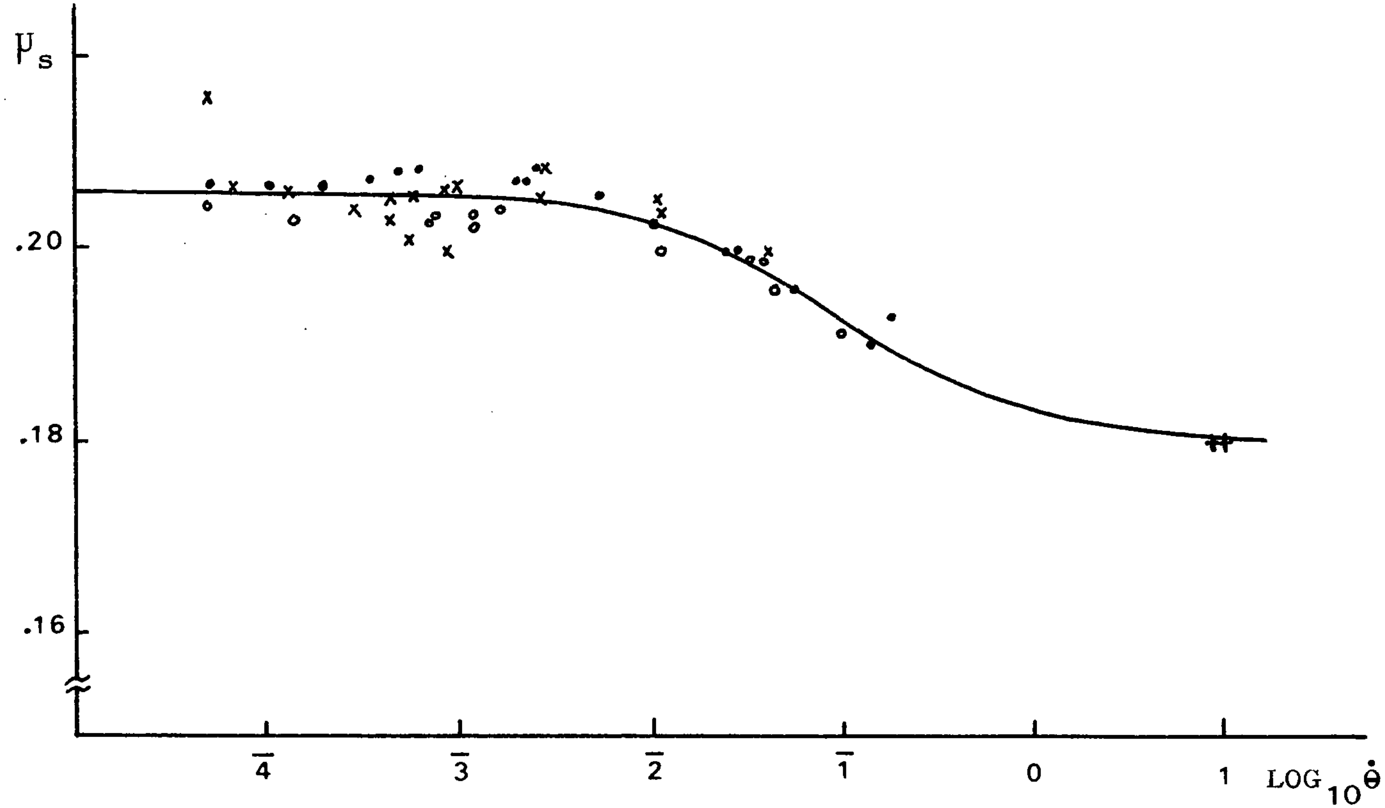

FIG. 4-17 μ_s VERSUS $LOG_{10}\dot{\theta}$ — PYRITE WITH LUBRICANT (L.P.)

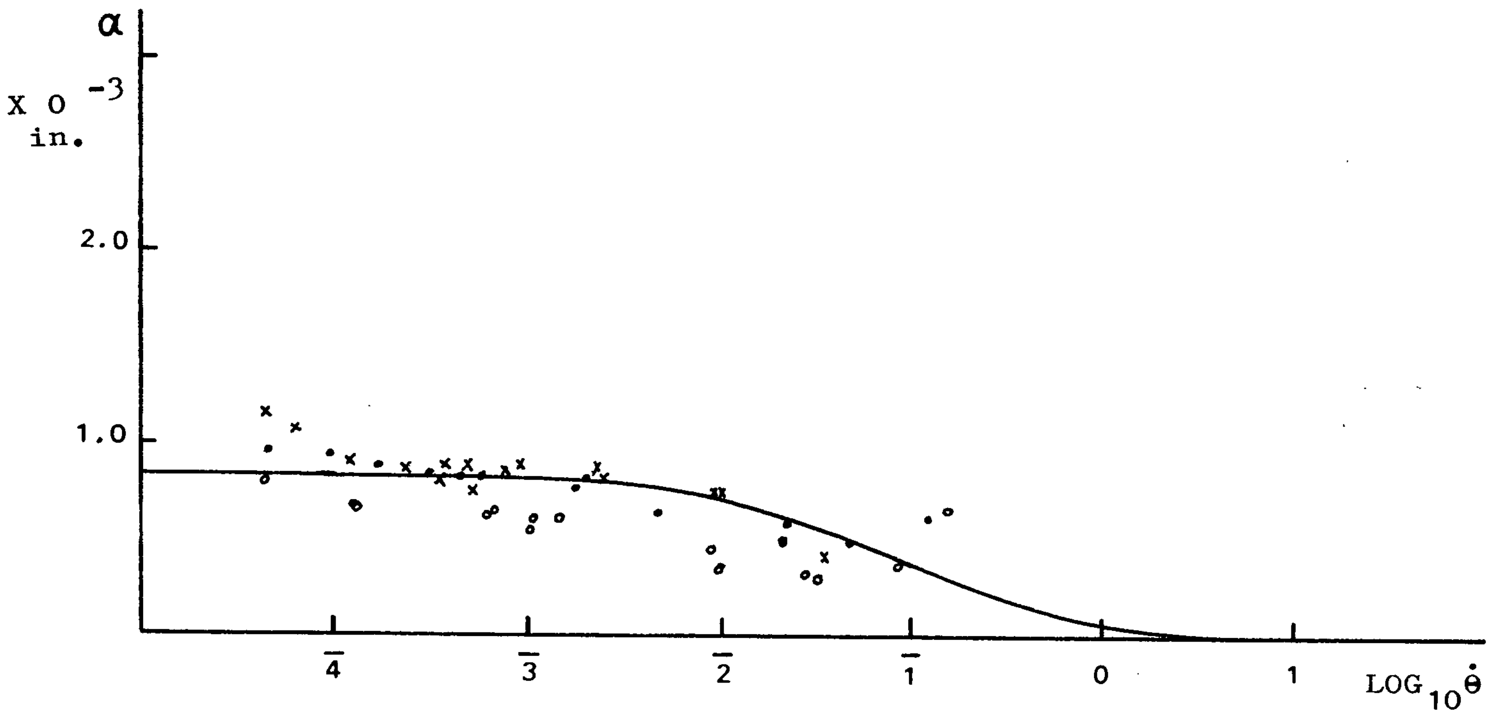

FIG. 4-18 α VERSUS $\mathrm{LOG}_{10}\dot{\theta}$ —— PYRITE WITH LUBRICANT

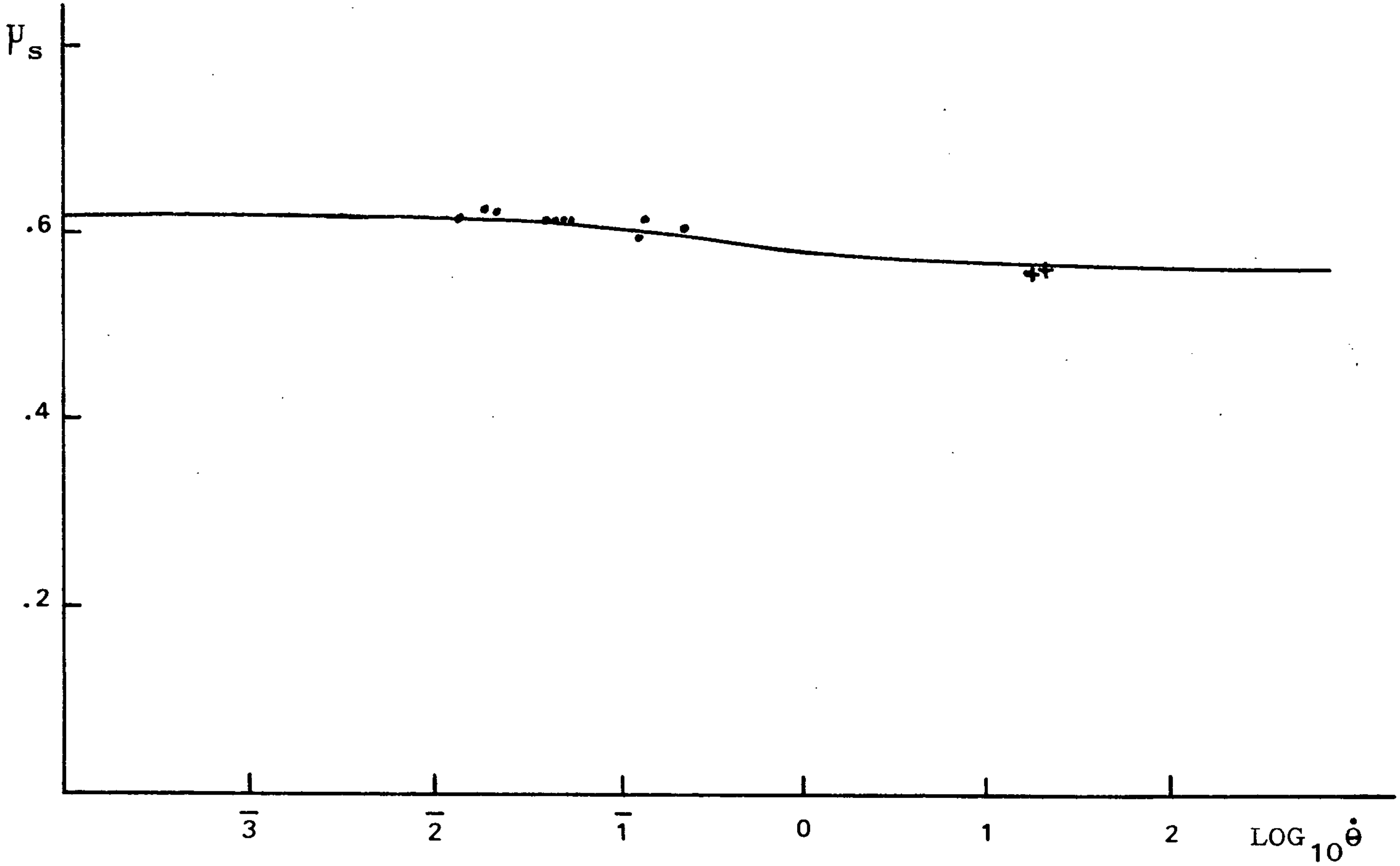

FIG. 4-19 μ_s VERSUS $LOG_{10}\dot{\theta}$ — WET BLACK MARBLE

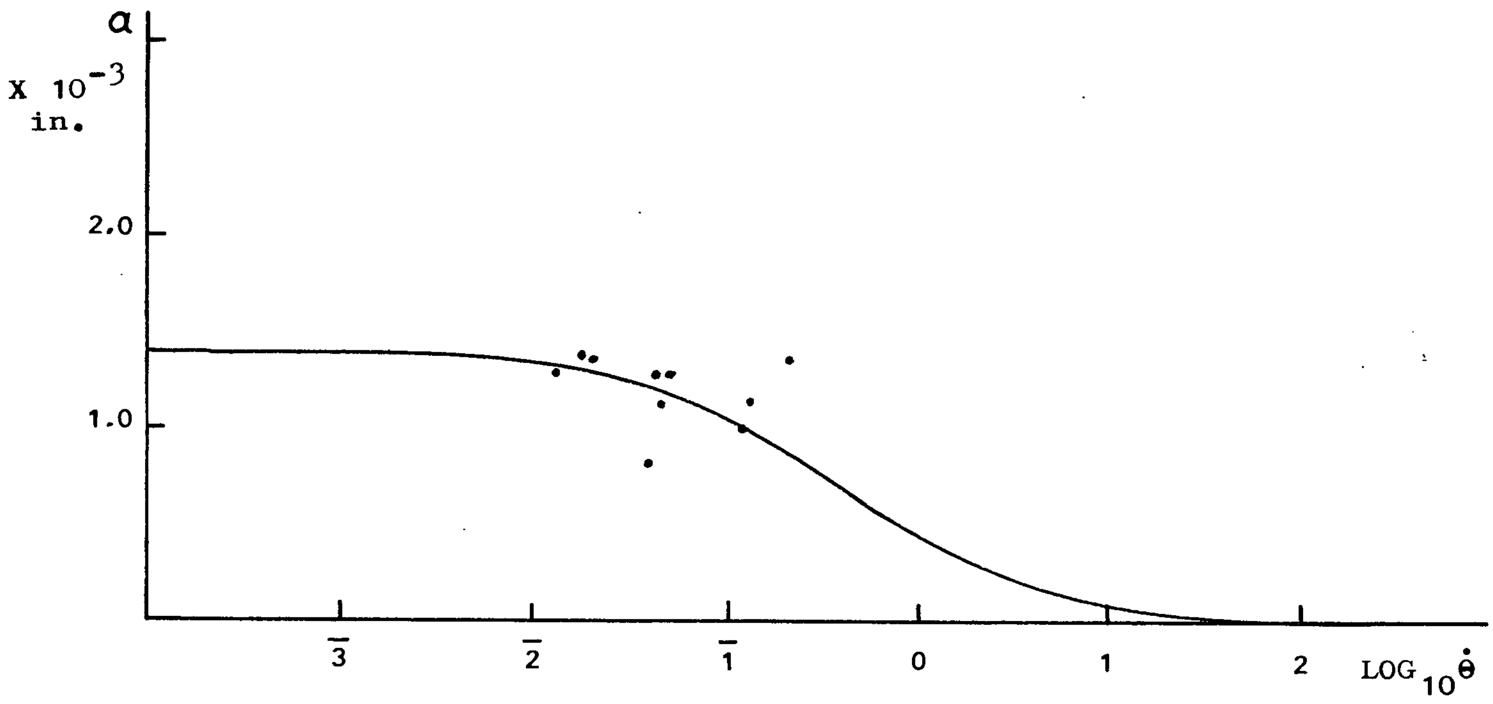

FIG. 4-20 α VERSUS $LOG_{10}\dot{\theta}$ — WET BLACK MARBLE

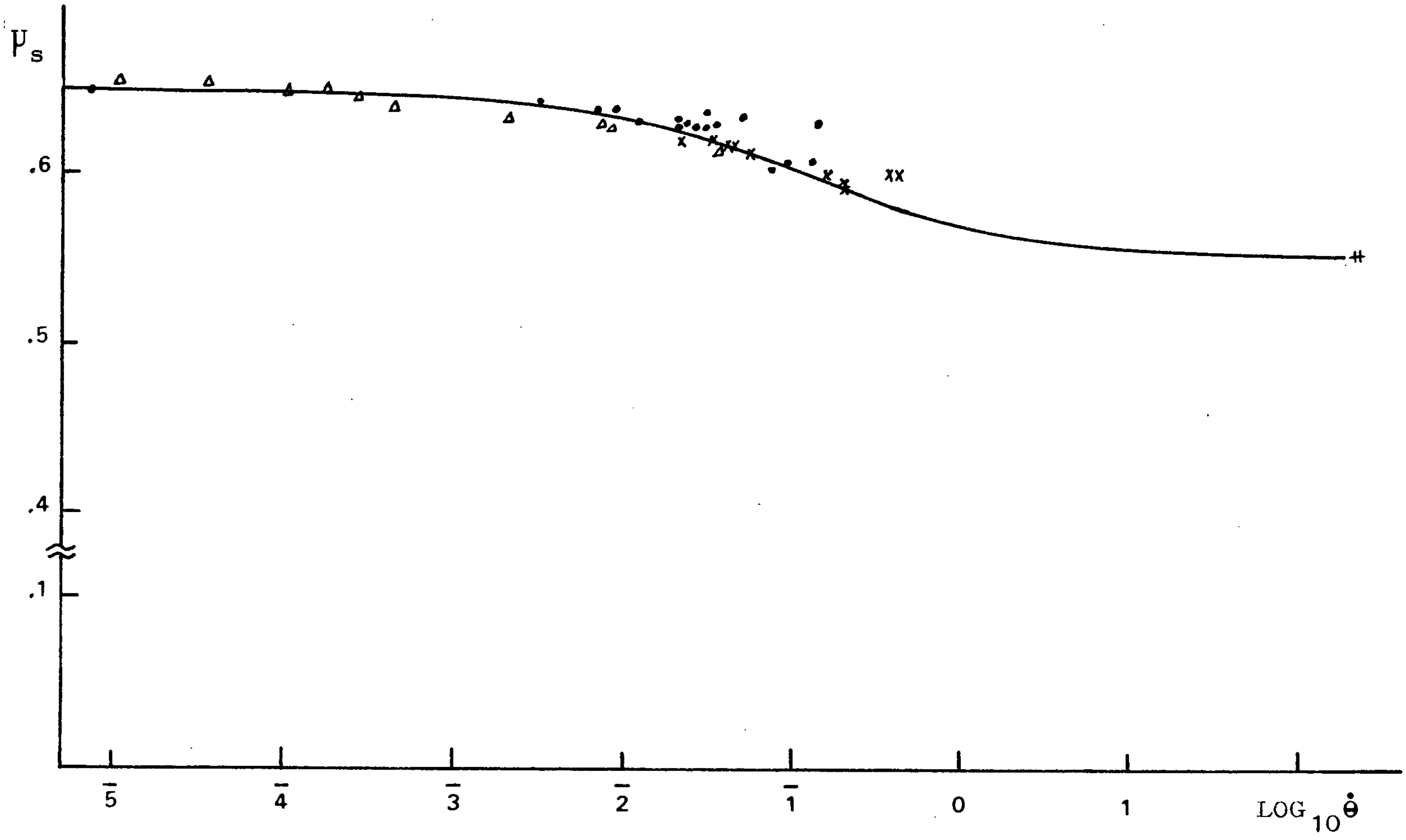

FIG. 4-21 μ_s VERSUS $\mathrm{LOG}_{10}\dot{\theta}$ — WET GRANODIORITE

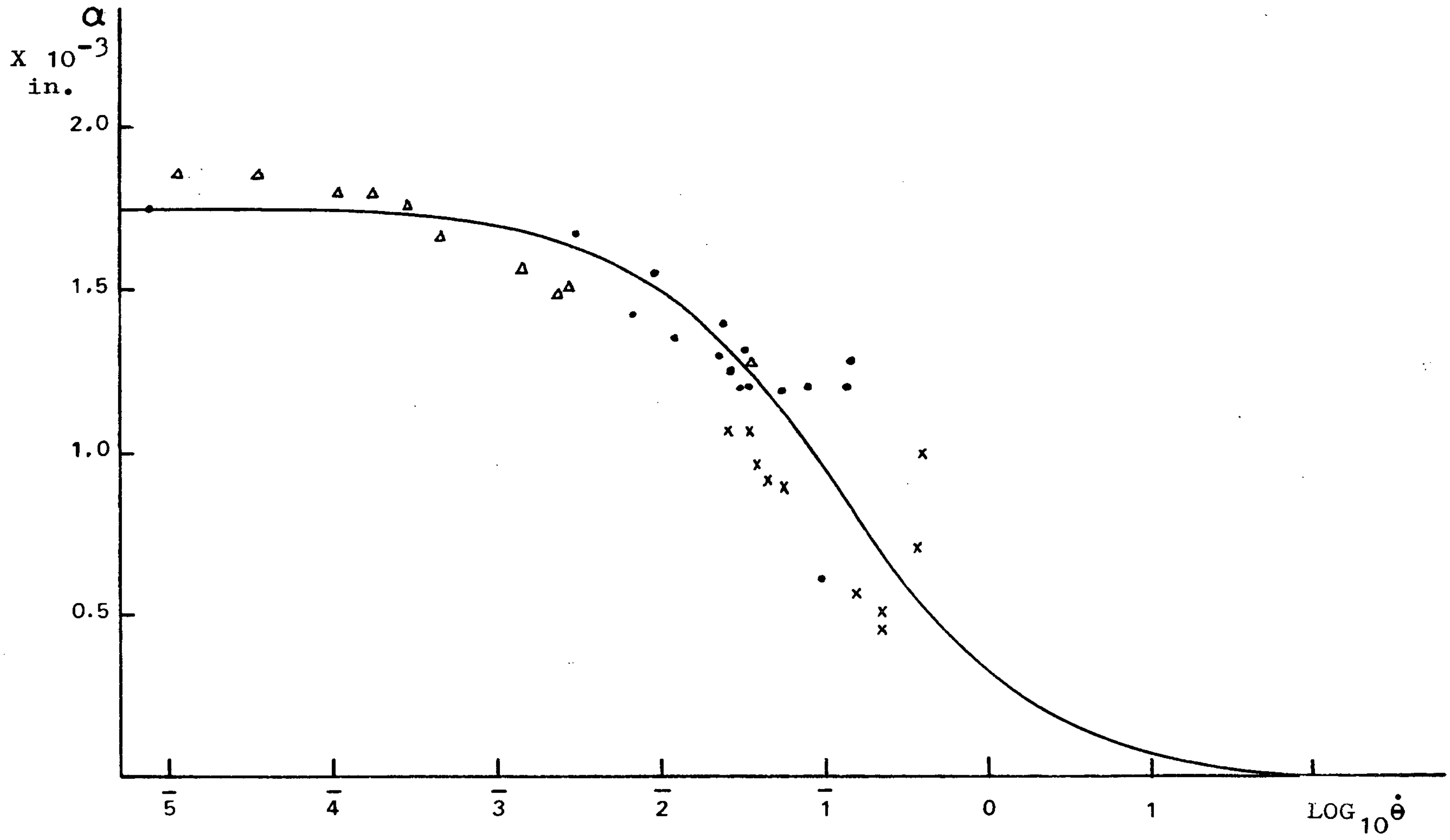

FIG. 4-22 α VERSUS $\text{LOG}_{10}\dot{\theta}$ —— WET GRANODIORITE

TABLE I: PARAMETERS OF EXPERIMENTAL SYSTEMS AND THE THEORY

Fig.	W (lb)	K (10^4 lb/in)	a	b	c	d	A_o (10^{-2} in)	μ_{so}	μ_m	Fig.
1, 2	225.8	1.94	9.09	263.6	2.607	1.130	2.325	0.30	0.19	1, 2
3, 4	224.5	1.94	10.0	66.1	1.322	.5745	2.315	0.56	0.46	3, 4
5, 6	224.5	1.94	7.15	18.26	1.533	0.665	2.315	0.53	0.39	5, 6
7, 8	137.8	1.94	7.699	12800	3.307	1.434	1.42	0.85	0.72	7, 8
9, 10	137.8	1.94	3.703	.003107	3.807	1.653	1.42	0.92	0.65	9, 10
11, 12	181.2	1.94	4.35	42.5	1.553	0.674	1.87	0.38	0.15	11, 12
13, 14	430.6	1.94	62.5	2432.	1.281	0.5565	4.44	0.326	0.310	13, 14
15, 16	430.6	1.94	125.0	3375.	1.10	0.478	4.44	0.226	0.218	15, 16
17, 18	310.0	1.94	38.45	283.2	1.908	0.828	3.195	0.206	0.180	17, 18
19, 20	224.5	1.94	16.67	34.4	1.946	0.845	2.315	0.62	0.56	19, 20
21, 22	169.9	1.94	10.00	38.0	1.532	0.665	1.751	0.65	0.55	21, 22

NOTE: $$\mu_s = \frac{1}{a + b\dot{\theta}^d} + \mu_m = \frac{1}{a + be^{c(\log_{10}\dot{\theta})}} + \mu_m$$

$$\alpha = A_o(\mu_s - \mu_m)$$

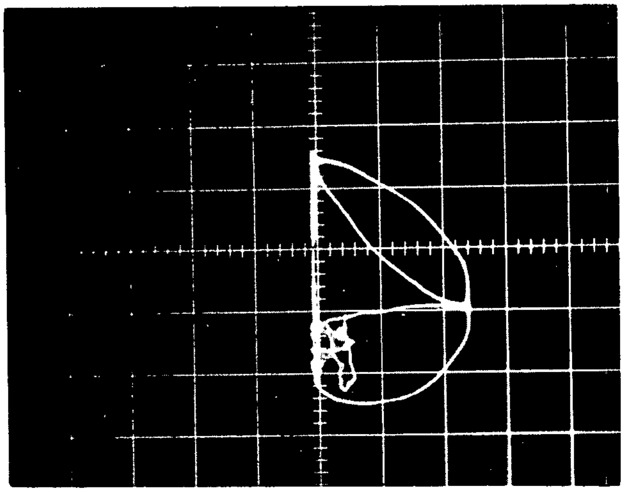

Scale: Force 1 Div = 9.7 lbs
Displacement 1 Div = 0.0005 in
Velocity 1 Div = 0.104 in/sec

FIG. 4-23 PHASE PLANE DIAGRAM OF STEEL

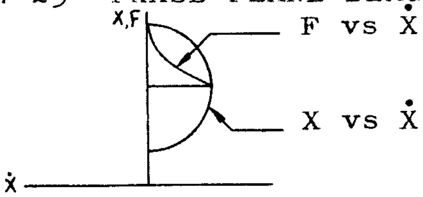

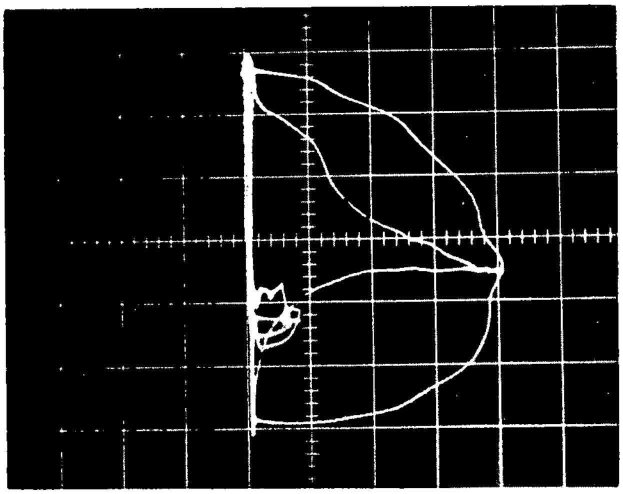

Scale: Force 1 Div = 9.7 lbs
Displacement 1 Div = 0.0005 in
Velocity 1 Div = 0.0635 in/sec

FIG. 4-24 PHASE PLANE DIAGRAM OF GLASS

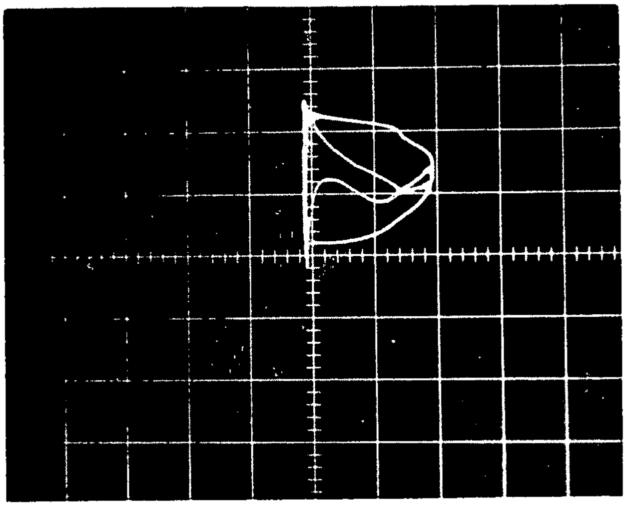

	Force	1 Div = 7.76 lbs
Scale:	Displacement	1 Div = 0.0004 in
	Velocity	1 Div = .0373 in/sec

FIG. 4-25 PHASE PLANE DIAGRAM OF PYRITE

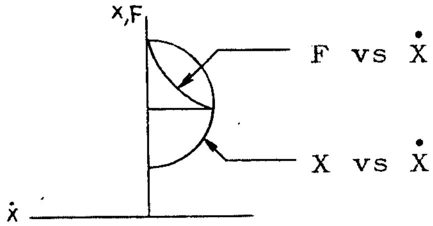

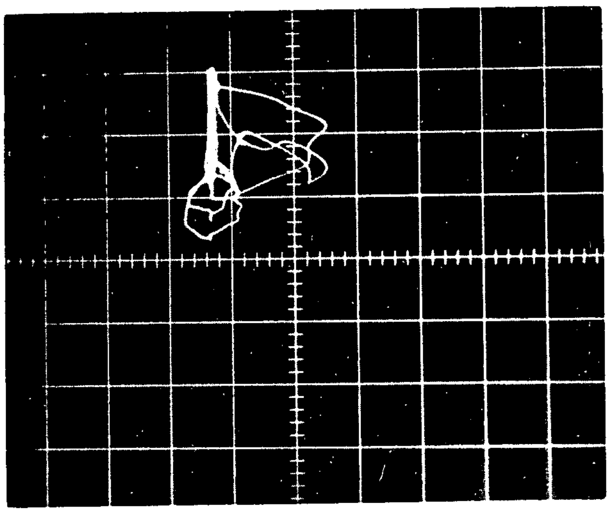

	Force	1 Div = 15.12 lbs
Scale:	Displacement	1 Div = 0.00078 in
	Velocity	1 Div = 0.084 in/sec

FIG. 4-26 PHASE PLANE DIAGRAM OF BLACK MARBLE

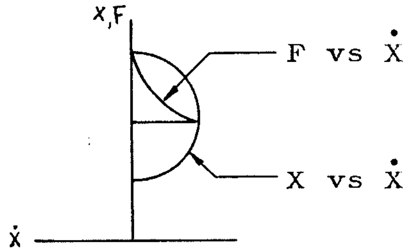

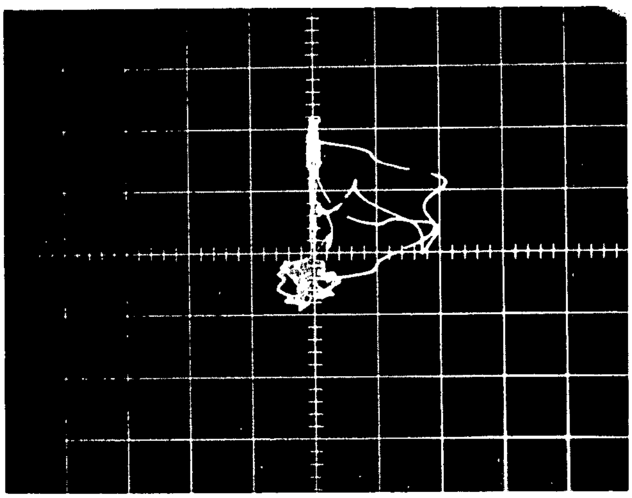

Scale:	Force	1 Div = 13.2 lbs
	Displacement	1 Div = 0.00068 in
	Velocity	1 Div = 0.933 in/sec

FIG. 4-27 PHASE PLANE DIAGRAM OF GRANODIORITE

CHAPTER V

DISCUSSION

5-1. LABORATORY RESULTS:

The purpose of the present work was to study the stick-slip vibrations of rock systems with the objective of applying the results to earthquake mechanics. A theoretical analysis was made to relate the amplitude of vibration to the frictional and other properties of the system. This analysis showed that the amplitude of stick-slip was proportional to the difference between μ_s and μ_m, and diminished as velocity increased. The approximate equation arising from this analysis was found to be

$$\alpha = \frac{W}{K}\left(\frac{1}{\frac{1}{\mu_{so} - \mu_m} + b\dot{\theta}^d} \right)(1 + e^{-\lambda\pi})$$

The results of the present experimental work are presented in chapter four. Theoretical curves based on equation (2-19) were also plotted in order to compare theory with experiment. The comparison indicated two facts. First, equation (2-18) describing the μ-$\dot{\theta}$ relationship was valid for both metals and non-metals. This result suggested that, even though rocks are considered to be brittle, their frictional behaviour is similar to that of metal. Second, the amplitude results fit the theory with reasonable agreement indicating that the present analysis was valid for the prediction of the amplitude of stick-slip vibration.

The experimental results also suggested that the coefficient of friction and the amplitude of stick-slip vibration of rocks would be affected by the porosity and the ductility of the material. The porosity of a material is a ratio of the volume of pores within the material to the bulk volume of the material. The mechanical properties of the material are influenced by internal spaces in the structure and the strength of rock is reduced when it is immersed in water. If the bulk strength is altered by water then some influence on frictional values might be expected. The addition of water on pyrite and black-marble lowered the frictional value to 60% of its original value, but gave no change with steel and glass. Mineral oil lowered the coefficient of friction of all specimens to about 60% of original values.

The effect of water on the stick-slip amplitude of rock material was not unique. It caused granodiorite to possess stick-slip from stable sliding, but reduced the stick-slip amplitude of pyrite. When the properties of the rocks were considered, the above results implied that the amplitude of stick-slip vibration of igneous or low porosity rocks would be increased and that of sedimentary or high porosity rocks would be decreased if water was introduced into the rubbing system.

Ductility is defined as the ability of material to deform permanently without fracture (36). The ductilities of pyrite and black-marble under fairly low hydrostatic pressure, were found (36) to be 0.5% and over 20% respectively, and the ductility of 1020 steel was much higher than these values. The experimental results indicated that the difference between μ_{so} and μ_m of wet pyrite, dry pyrite, black-marble, steel with petrolatum and dry steel were 0.008, 0.02, 0.06, 0.1 and 0.2 respectively. The coincidence of the increase of the difference between μ_{so} and μ_m with the ductility of material suggested that the amplitude of stick-slip vibration might be a function of ductility.

5-2. APPLICATION TO EARTHQUAKE MECHANICS:

The mechanics of earthquake fault displacements will be considered. Wilson (37) in 1965 stated that the shear stress at opposite sides of a strike-slip fault was generated by tectonic divergent ridges as shown in Fig. 5-1.

A number of shallow earthquakes have occurred at strike-slip fault zones. The San Andreas fault, having a total length of about 600 miles (38), has a typical strike-slip fault zone. In the April, 1906 San Francisco earthquake (39,40) the displacement was entirely horizontal and the fault was active over a length of 270 miles during the earthquake. Permanent displacement as large as 21

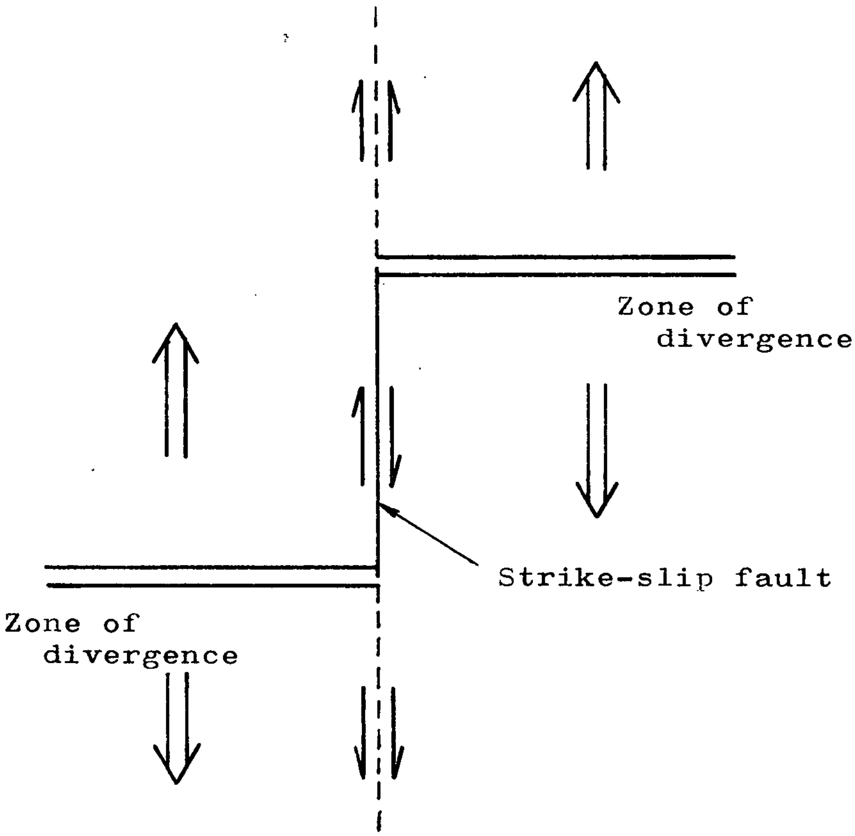

FIG. 5-1 STRIKE-SLIP FAULT MECHANISM

feet were observed along the fault and the displacement diminished as the transverse distance from the fault became greater. This decrease in permanent deformation at increased distances from the fault implied that an elastic zone existed on each side of the fault prior to the displacement. The width of this elastic zone was thought to be as wide as 10 kilometers on each side of the fault (40). The epicenter, the fault trace and the geologic structure of the fault are shown in Fig. 5-2 (41). The geology consisted mainly of highly disturbed and slightly metamorphosed sediments of the Franciscan series and adjacent granitic rocks. Granitic rock is the basic rock that lays underneath the surface structure and this granitic foundation joins the coastal system to the granitic structure in Sierra Nevada (39). In the active zone of the San Andreas fault, it was reported that the slip-rate of the ground along the fault was about two inches per year (35). Generally, large earthquakes occur mostly in inactive zones. If the slip-rate was uniform throughout the whole length of the fault then elastic strain would build up in the inactive zone year after year because the rate of the displacement outside the elastic zone would equal the slip-rate in the active zone.

When the width of elastic zone is compared with the length of the fault, it is possible to approximate the elastic zone by the pure shear model as shown in Fig. 5-3 (40). This system could be simplified as a single-degree-of-freedom vibrational system as shown in Fig. 5-4.

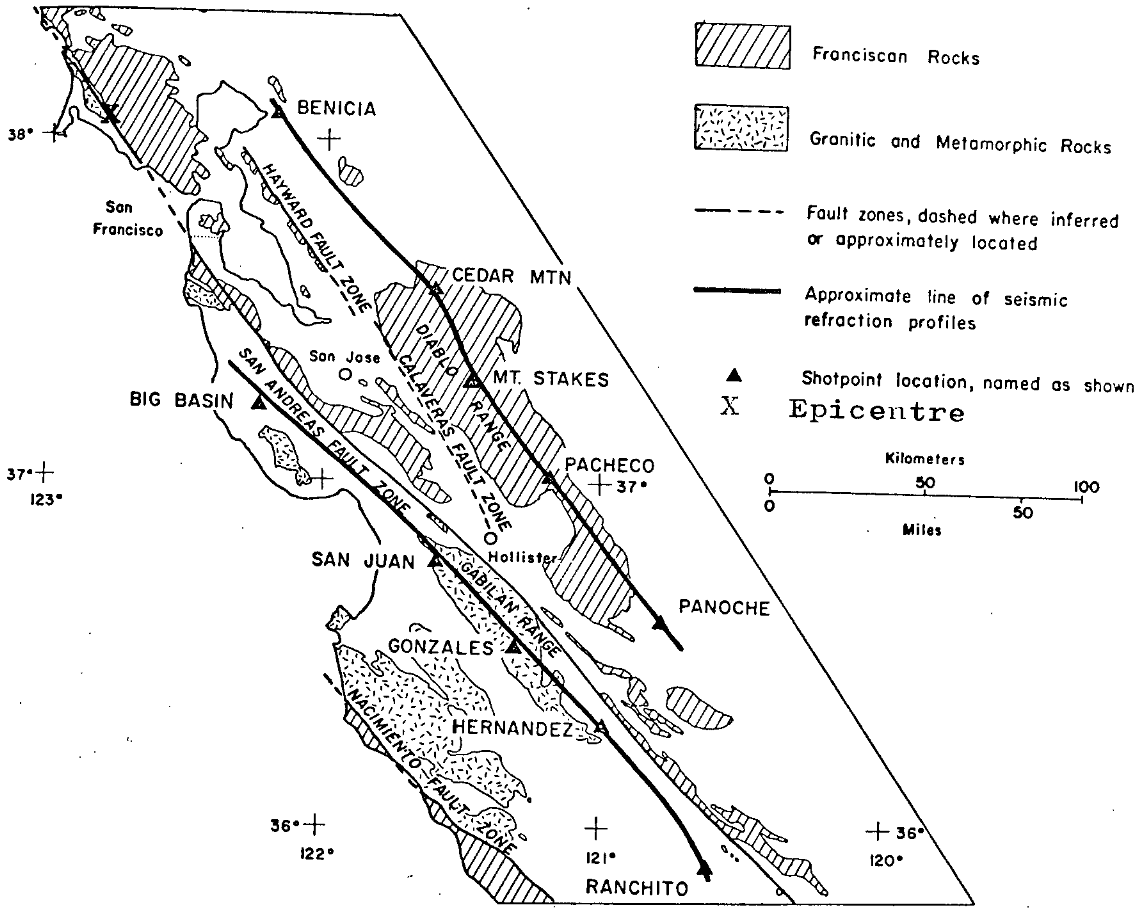

Fig. 5-2 Index Map of Shotpoints and Seismic Profiles in the Gabilan and Diablo Ranges, Central California.

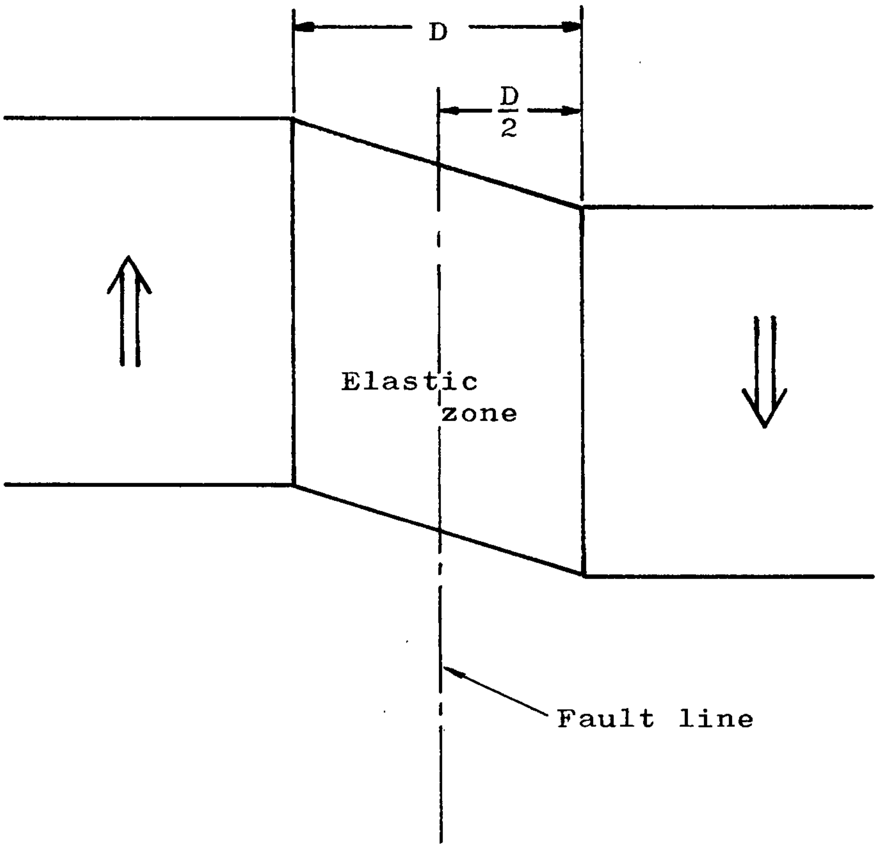

FIG. 5-3 A PURE SHEAR MODEL OF ELASTIC ZONE

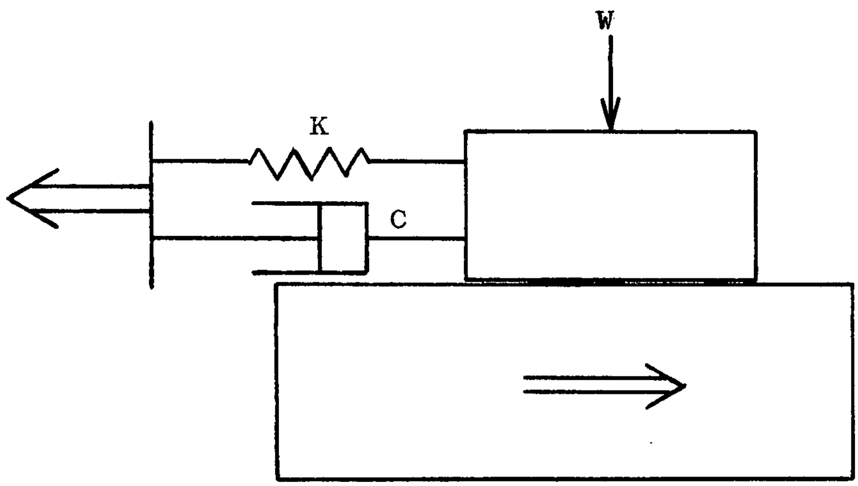

FIG. 5-4 MODEL OF AN EARTHQUAKE VIBRATION SYSTEM

The amplitude of the stick-slip vibration of a system similar to Fig. 5-4 was given by equation (2-19):

$$\alpha = \frac{W}{K}\left(\frac{1}{\frac{1}{\mu_{so} - \mu_m} + b\dot{\theta}^d} \right)(1 + e^{-\lambda\pi}) \qquad (5\text{-}1)$$

For $\dot{\theta} << 1$ and small damping the equation reduces to

$$\alpha = \frac{W}{K}(\mu_{so} - \mu_m)(2) \qquad (5\text{-}2)$$

and the equivalent stiffness of the system is given by

$$K = \frac{G}{D} \qquad (5\text{-}3)$$

Therefore,

$$\alpha = \frac{2WD}{G}(\mu_{so} - \mu_m) \qquad (5\text{-}4)$$

where G is the shear modulus of the geological material.

Brune, Henyey and Roy (42) suggested that the upper limit of initial stress at a rate of 5 cm/year would be 250 bars. Assume that the geology of the fault was granodiorite which has $\mu_{so} = 0.65$ then the equivalent normal load becomes:

$$W = \frac{250 \text{ bars}}{0.65} = 385 \text{ bars}$$

Using D = 13 miles (40), $G = 0.25 \times 10^6$ bars (36)

$$K = \frac{G}{D} = \frac{0.25 \times 10^6 \times 14.5 \text{ psi}}{13 \times 63360 \text{ in}} = 4.4 \text{ psi/in}$$

Using a load-rate of 2 in/year (35) gives,

$$\dot{\theta} = \frac{KV}{W} = \frac{4.4 \times 2}{14.5 \times 385 \times 365 \times 24 \times 3600} \text{ sec}^{-1}$$

$$= 5 \times 10^{-10} \text{ sec}^{-1}$$

The results for granodiorite in chapter four gave:

$$\mu_{so} = 0.65$$

$$\mu_m = 0.55$$

Substitution into equation (5-4) yields

$$\alpha = \frac{2W}{K}(\mu_{so} - \mu_m)$$
$$= \frac{2 \times 385 \times 14.5}{4.4}(0.65 - 0.55) \text{ inches}$$
$$= 254 \text{ inches}$$

or $\alpha = 21.2$ feet

If we consider that the geologic structure at the fault to be granodiorite, it would give a horizontal displacement of about 21 feet. This displacement is nearly the same as the displacement reported for the 1906 disturbance.

Consider the rock structure to be granite. G for granite is 0.2×10^6 bars (36).

$$K = \frac{G}{D} = \frac{0.2 \times 10^6 \times 14.5 \text{ psi}}{13 \times 63360 \quad \text{in}} = 3.52 \text{ psi/in}$$
$$\dot{\theta} = \frac{KV}{W} = \frac{3.52 \times 2}{14.5 \times 385 \times 365 \times 24 \times 3600} \text{ sec}^{-1}$$
$$= 4 \times 10^{-10} \text{ sec}^{-1}$$

Choosing the horizontal displacement as 21 feet, gives

$$\mu_{so} - \mu_m = \frac{\alpha K}{2W} = \frac{21 \times 12 \times 3.25}{2 \times 385 \times 14.5} = 0.079$$

and
$$\mu_{so} = \frac{F_f}{W} = \frac{250 \text{ bars}}{385 \text{ bars}} = 0.65$$

therefore,

$$\mu_m = 0.65 - 0.079 = 0.57$$

This calculation suggests that the kinetic coefficient of friction of granite would be 0.57.

In conclusion, if the shallow earthquake movement is analogous to stick-slip vibration, then it would appear that reasonable estimates of fault displacement are possible. If the geology and the slip-rate of the fault are known, the amplitude of the earthquake can be predicted. In addition, the period of the fault displacements can be estimated as:

$$T = \frac{\alpha}{\dot{\varepsilon}} = \frac{WD}{\dot{\varepsilon} G}(\mu_{so} - \mu_m)(2)$$

$$= \frac{2WD}{\dot{\varepsilon} G}(\mu_{so} - \mu_m) \qquad (5\text{-}5)$$

where T is the period of disturbance and $\dot{\varepsilon}$ is the slip-rate applied along the fault.

CHAPTER VI

6-1. CONCLUSIONS:

The friction induced vibration of four types of rock have been investigated. Glass and steel were also used for the purpose of comparing the frictional behaviour of rocks to that of other materials.

To summarize the present work the following results have been obtained.

(1) The hydraulically driven apparatus provided good friction results in the very low velocity range. A velocity range from 10^{-6} in/sec to 2 in/sec was easily achieved.

(2) A μ_s-$\dot{\theta}$ equation was found in the following form,

$$\mu_s = \frac{1}{\frac{1}{\mu_{so} - \mu_m} + b\dot{\theta}^d} + \mu_m$$

which was found to be applicable for both metals and non-metals. The results which fitted this equation also suggested that there was no discontinuity between static and kinetic coefficients of friction.

(3) Under several conditions relaxation oscillations were achieved for all specimens except green schist and granodiorite. Green schist gave no obvious stick-slip but a fairly constant μ of about 0.66 when dry and 0.55 when wet. On the other hand granodiorite did not show oscillation when dry but produce vibrations when

wet.

(4) The friction and amplitude results as plotted in chapter four, gave good agreement with theoretical curves. The frictional behaviour of metals and non-metals appeared to be very similar.

(5) Water was a good lubricant for some rocks suggested that the friction of rocks might be a function of the porosity of the material.

(6) Mineral oil was a good lubricant not only for metal but also for rocks and glass. This suggested that the effect of mineral oil on the surface conditions of metal and non-metal was the same.

(7) The amplitudes of vibration of the surfaces tested appeared to correlate with the ductility of the materials. It was believed that ductility might be one of the factors governing the size of vibration amplitude.

(8) An approximate calculation based on the known conditions found in an earthquake zone gave an amplitude of earthquake vibration very close to the maximum permanent displacement measured along the earthquake fault zone. This calculation supported Brace and Byerlee's suggestion that frictional stick-slip oscillations might be the mechanism of earthquakes.

(9) The amplitude of vibration was found from the equation

$$\alpha = \frac{W}{K}\left(\frac{1}{\frac{1}{\mu_{so} - \mu_m} + b\dot{\theta}^d} \right)(1 + e^{-\lambda\pi})$$

An estimate of the period of earthquakes is given by

$$T = \frac{2WD}{\dot{\varepsilon}G}(\mu_{so} - \mu_m)$$

6-2. RECOMMENDATIONS:

(1) Friction measurements at high driven velocity were limited by the present apparatus. To obtain friction results at high $\dot{\theta}$, an apparatus with a wider velocity range should be used.

(2) From the mechanical point of view, friction tests under uniaxial stress were used. However, for studies in the field of rock mechanics, hydrostatic pressure should be considered. The hydrostatic pressure in the triaxial stress state is commonly obtained by surrounding the test specimens with pressurized fluid. In order to provide a triaxial stress state, the present apparatus would require extensive redesign.

(3) The present experiments were made at room temperature, whereas at depths of about 10 kilometers the temperature would be considerably higher. The effect of varying temperature should be considered when rock friction is investigated further.

APPENDIX I

DETERMINATION OF CRITICAL $\dot{\theta}$:

Consider the case when V is at critical, that is at V_c. There must exist the following conditions:

$$x_o = \frac{W}{K}\mu_{sc} \tag{I-1}$$

where μ_{sc} is the static coefficient of friction at V_c.

$$\dot{x}_o = V_c \tag{I-2}$$

From equation (2-13):

$$x_3 = \frac{W}{K}\mu_m - \frac{C}{K}V_c \tag{I-3}$$

$$\dot{x}_3 = V_c \tag{I-4}$$

$$\ddot{x}_3 = 0 \tag{I-5}$$

Choosing t = 0 at point 0 in Fig. I-1,

and $t = t_3$ at point 3.

From equation (2-9):

$$x_o = \frac{W}{K}(\mu_m + \beta V_c) + A \tag{I-6}$$

$$x_3 = \frac{W}{K}(\mu_m + \beta V_c) + e^{-\lambda\omega_d t_3}\left[A\cos\omega_d t_3 + B\sin\omega_d t_3\right] \tag{I-7}$$

From equation (2-10):

$$\dot{x}_o = \omega_d(B - \lambda A) \tag{I-8}$$

$$\dot{x}_3 = \omega_d e^{-\lambda\omega_d t_3}\left[(B - \lambda A)\cos\omega_d t_3 - (A + \lambda B)\sin\omega_d t_3\right] \tag{I-9}$$

From equation (2-11):

$$\ddot{x}_3 = -\omega_d^{\,2} e^{-\lambda\omega_d t_3}\left\{\left[A(1 - \lambda^2) + 2\lambda B\right]\cos\omega_d t_3 + \left[B(1 - \lambda^2) - 2\lambda A\right]\sin\omega_d t_3\right\} \tag{I-10}$$

Substitute equation (I-2) into equation (I-8):

$$B = \frac{V_c}{\omega_d} + \lambda A \tag{I-11}$$

Substitute equations (I-3) and (I-11) into equation (I-7) and simplify:

$$\frac{-V_c(C + W\beta)}{K}e^{\lambda\omega_d t_3} = \left[A\cos\omega_d t_3 + (\frac{V_c}{\omega_d} + \lambda A)\sin\omega_d t_3\right] \tag{I-7a}$$

Substitute equations (I-4) and (I-11) into equation (I-9) and simplify:

$$\frac{V_c}{\omega_d}e^{\lambda\omega_d t_3} = (\frac{V_c}{\omega_d})\cos\omega_d t_3 - \left[A(1 + \lambda^2) + \frac{V_c}{\omega_d}\right]\sin\omega_d t_3 \tag{I-9a}$$

Substitute equations (I-5) and (I-11) into equation (I-10) and simplify:

$$0 = \left[A(1 + \lambda^2) + 2\lambda\frac{V_c}{\omega_d}\right]\cos\omega_d t_3 + \left[\frac{V_c}{\omega_d}(1 - \lambda^2) - \lambda A(1 + \lambda^2)\right]\sin\omega_d t_3 \tag{I-10a}$$

and also:

$$\omega_d t_3 = \tan^{-1}\left[\frac{A(1 + \lambda^2) + 2\lambda\frac{V_c}{\omega_d}}{\frac{V_c}{\omega_d}(1 - \lambda^2) - \lambda A(1 + \lambda^2)}\right] \tag{I-12}$$

Let $H = \frac{V_c}{\omega_d}$, simplify equation (I-7a) with equation (I-9a):

$$A\cos\omega_d t_3 + (H + \lambda A)\sin\omega_d t_3 = \frac{-\omega_d(C + W\beta)}{K}\left\{H\cos\omega_d t_3 - \left[A(1 + \lambda^2) + H\right]\sin\omega_d t_3\right\}$$

Let $P = \frac{\omega_d(C + W\beta)}{K}$, and the above equation becomes

$$(A + PH)\cos\omega_d t_3 = \left\{P\left[A(1 + \lambda^2) + H\right] - (H + \lambda A)\right\}\sin\omega_d t_3$$

or

$$\omega_d t_3 = \tan^{-1}\left\{\frac{A + PH}{P\left[A(1 + \lambda^2) + H\right] - (H + \lambda A)}\right\} \tag{I-13}$$

Equation (I-12) and equation (I-13) must be equal.

Therefore,

$$\frac{A(1 + \lambda^2) + 2\lambda H}{H(1 - \lambda^2) - A\lambda(1 + \lambda^2)} = \frac{A + PH}{P\left[A(1 + \lambda^2) + H\right] - \left[H + \lambda A\right]}$$

The above equation con be simplified to give a quadratic equation in A:

$$A^2P(1 + \lambda^2)^2 + AH(3P\lambda + P - 2)(1 + \lambda^2) + H^2\left[P(\lambda^2 + 2\lambda - 1) - 2\lambda\right] = 0 \qquad \text{(I-14)}$$

Therefore,

$$A = \frac{V_c}{2P(1 + \lambda^2)\omega_d}R \qquad \text{(I-15)}$$

where:

$$R = (2 - P - 3\lambda P) \pm \left[5P^2\lambda^2 - 2P(P + 2)\lambda + (5P^2 - 4P + 4)\right]^{\frac{1}{2}}$$

A is real therefore R must be real, that is:

$$5P^2\lambda^2 - 2P(P + 2)\lambda + (5P^2 - 4P + 4) > 0 \qquad \text{(I-16)}$$

Inequality (I-16) is a condition that restricts the variability of system parameters.

Substitute equation (I-15) into equation (I-6),

$$x_o = \frac{W(\mu_m + \beta V_c)}{K} + \frac{V_c}{2P(1 + \lambda^2)\omega_d}R \qquad \text{(I-17)}$$

Consider equation (2-18) in chapter two:

$$\mu_s = \frac{1}{\frac{1}{\mu_{so} - \mu_m} + b\dot{\theta}^d} + \mu_m \qquad \text{(I-18)}$$

Equation (I-1) becomes

$$x_o = \frac{W}{K}\left[\frac{1}{\frac{1}{\mu_{so} - \mu_m} + b\dot{\theta}_c^d} + \mu_m\right] \qquad \text{(I-19)}$$

Equation (I-16) must satisfy the boundary condition in equation (I-19):

$$\frac{W}{K}\mu_m + \left[\frac{W}{K}\beta + \frac{R}{2P(1 + \lambda^2)\omega_d}\right]V_c =$$

$$\frac{W}{K}\left[\frac{1}{\frac{1}{\mu_{so} - \mu_m} + b\dot{\theta}_c^d} + \mu_m\right] \tag{I-20}$$

From equation (2-3):

$$V_c = \frac{W}{K}\dot{\theta}_c$$

therefore,

$$\left[\frac{W}{K}\beta + \frac{R}{2P(1 + \lambda^2)\omega_d}\right]\dot{\theta}_c = \frac{1}{\frac{1}{\mu_{so} - \mu_m} + b\dot{\theta}_c} + \mu_m \tag{I-21}$$

Let $Z = \left[\frac{W}{K}\beta + \frac{R}{2P(1 + \lambda^2)\omega_d}\right]^{-1}$

therefore,

$$b\dot{\theta}_c^{d+1} + \frac{1}{\mu_{so} - \mu_m}\dot{\theta}_c - Z = 0 \tag{I-22}$$

If the parameters of the vibrating system are known critical $\dot{\theta}$ can be found from equation (I-22). That is, equation (I-22) can be used to predict whether vibration occurs or not.

REFERENCES

1. Wells, J.H., "Kinetic Boundary Friction", The Engineer (London), Vol. 147, p. 454, 1929.

2. Kaidanovskii, N.L. and Khaikin, B.E., Journal of Technical Physics, U.S.S.R., Vol. 3, p. 91, 1933.

3. Bowden, F.P. and Leben, L., "The Nature of Sliding and the Analysis of Friction", Proceedings of the Royal Society, Series A, Vol. 169, p. 371, 1939.

4. Bowden, F.P., Moore, A.C. and Tabor, D., Journal of Applied Physics, Vol. 14, p. 80, 1943.

5. Bristow, J.R., "Kinetic Boundary Friction", Proceedings of the Royal Society, Vol. 189, p. 88, 1945.

6. Lienard, A., "Etude des Oscillations Entretenues", Rev. Gen. Elect., Vol. 23, p. 901, 1928.

7. Dudley, B.R. and Swift, H.W., "Friction Relaxation Oscillations", The Philosophical Magazine, London, Series 7, Vol. 40, p. 849, 1949.

8. Rabinowicz, E., "The Nature of the Static and Kinetic Coefficients of Friction", Journal of Applied Physics, Vol. 22, No. 11, p. 1373, 1951.

9. Rabinowicz, E., "A Study of the Stick-Slip Process", Proceedings of the Symposium on Friction and Wear, Detroit, p. 149, 1957.

10. Derjagin, B.V., Push, V.E. and Tolstoi, D.M., "A Theory of Stick-Slip Sliding of Solids", Proceedings of the Conference on Lubrication and Wear, p. 257, Oct. 1957.

11. Singh, B.R., "A Study of Critical Velocity of Stick-Slip Sliding", Trans. A.S.M.E., Journal of Engineering for Industry, p. 393, Nov. 1960.

12. Potter, A.F., "A Study of Friction Induced Vibrations", M.A.Sc. Thesis in Mechanical Engineering, The University of British Columbia, 1963.

13. Cameron, R., "Friction Induced Vibration", M.A.Sc. Thesis in Mechanical Engineering, The University of British Columbia, 1963.

14. Johannes, V.I., "Friction Induced Vibrations in a Hydraulically Driven System", Ph.D. Thesis in Mechanical Engineering, The University of British Columbia, 1969.

15. Green, M.A., "Some Fundamental Aspects of Static Friction", M.A.Sc. Thesis in Mechanical Engineering, The University of British Columbia, 1971.

16. Marion, T.L., "Transitory Static and Kinetic Boundary Friction Mechanisms", Ph.D. Thesis in Mechanical Engineering, The University of British Columbia, 1972.

17. Bullen, K.E., An Introduction to the Theory of Seismology, Cambridge University Press, p. 1-3. 1947.

18. Dutton, C.E., Earthquakes, in the Light of the New Seismology, The Progressive Science Series, The Knickerbocker Press, New York, p. 6-9, 1904.

19. Reid, H.F., "The Elastic-Rebound Theory of Earthquakes", University of California Publications in Geology, Vol. 6, No. 19, p. 413, 1911.

20. Jeffreys, H., Earthquakes and Mountains, Methuen & Co. Ltd., London, p. 26, 1935.

21. Taylor, F.B., "Bearing of the Tertiary Mountain Belt on the Origin of the Earth's Plan", Bulletin of the Geological Society of America, 21(2), p. 179, June 1910.

22. Wegener, A., "The Origin of Continents and Oceans", Translated by John Biram, Dover Publication, Inc., New York, 1966.

23. Encyclopaedia Britannica, Vol. 21, p. 753, 1973.

24. Isacks, B., Oliver, J. and Sykes, L.R., "Seismology and the New Global Tectonics", Journal of Geophysical Research, Vol. 73, No. 18, p. 5855, Sept. 1968.

25. Orowan, E., "Mechanism of Seismic Faulting", Geological Society of America, Memoir, 79, p. 323, 1960.

26. Jaeger, J.C., "The Frictional Properties of Rock", Geofisica Pura e Applicata, Vol. 43, p. 148, 1959.

27. Griggs, D.T. et al., "Rock Deformation", Geological Society of America, Memoir, 79, p. 39, 1960.

28. Bridgman, P.W., "Shearing Phenomena at High Pressure", Proceedings, American Academy Arts and Sciences, Vol. 71, p. 387, 1936.

29. Brace, W.F. and Byerlee, J.D., "Stick Slip as a Mechanism for Earthquakes", Science, Vol. 153, p. 990, 1966.

30. Byerlee, J.D. and Brace, W.F., "Stick Slip, Stable Sliding and Earthquakes", Journal of Geophysical Research, Vol. 73, No. 18, p.6031, 1968.

31. Brace, W.F. and Byerlee, J.D., "California Earthquakes", Science, Vol. 168, p. 1573, 1970.

32. Drennon, C.B. and Handy, R.L., "Stick Slip of Lightly Loaded Limestone", Int. J. Rock Mech. Min. Sci., Vol. 9, p. 603, 1972.

33. Dieterich, J.H., "Time Dependent Friction in Rocks", Journal of Geophysical Research, Vol. 77, No. 20, p. 3690, 1972.

34. Ko, P.L., "Autonomous Quasi-Harmonic and Forced Vibration of Frictional System", Ph.D. Thesis in Mechanical Engineering, The University of British Columbia, 1969.

35. Whitten, C.A., "Measurements of Earth Movements in California", California, Division of Mines, Bulletin, 171, p. 75, 1955.

36. Clark, S.P., Handbook of Physical Constants, The Geological Society of America, Memoir 97, 1966.

37. Wilson, J.T., "A New Class of Faults and Their Bearing on Continental Drift", Nature, Vol. 207, No. 4995, p. 343, 1965.

38. Billings, M.P., Structural Geology, 3rd. ed., Prentice-Hall inc., New Jersey, p. 266, 1972.

39. Lawson, A.C., The California Earthquake of April 18, 1906, Report of the State Earthquake Investigation Commission, Vol. 1, 1908.

40. Reid, H.F., "The Mechanics of the Earthquake", The California Earthquake of April 18, 1906, Report of the State Earthquake Investigation Commission, Vol. 2, 1908.

41. Stewart, S.W., "Preliminary Comparison of Seismic Traveltimes ...", Proceedings of Conference on Geologic Problems of San Andreas Fault System, Stanford University Publication, Geological Sciences, Vol. XI, p. 219, Fig. 1, 1968.

42. Brune, J.N., Henyey, T.L. and Roy, R.F., "Head Flow, Stress and Rate of Slip along the San Andreas Fault, California", Journal of Geophysical Research, Vol. 74, No. 15, July 1969.